

การสังเคราะห์ซิลิคอนไนไตรด์พูนด้วยกระบวนการคาร์โบเทอร์มอลรีดักชันและไนไตรเคชันของ

ซิลิกา/อาร์เอฟเจล คอมพอสิต



นาย กนกศักดิ์ ลู่จิว

สถาบันวิทยบริการ

วิทยานิพนธ์นี้เป็นส่วนหนึ่งของการศึกษาตามหลักสูตรปริญญาวิศวกรรมศาสตรมหาบัณฑิต

สาขาวิชาวิศวกรรมเคมี ภาควิชาวิศวกรรมเคมี

คณะวิศวกรรมศาสตร์ จุฬาลงกรณ์มหาวิทยาลัย

ปีการศึกษา 2549

ลิขสิทธิ์ของจุฬาลงกรณ์มหาวิทยาลัย

POROUS SILICON NITRIDE SYNTHESIS VIA
THE CARBOTHERMAL REDUCTION AND NITRIDATION
OF SILICA/RF GEL COMPOSITE



Mr. Kanoksak Luyjew

สถาบันวิทยบริการ
จุฬาลงกรณ์มหาวิทยาลัย

A Thesis Submitted in Partial Fulfillment of the Requirements for the
Degree of Master of Engineering Program in Chemical Engineering

Department of Chemical Engineering

Faculty of Engineering

Chulalongkorn University

Academic Year 2006

Copyright of Chulalongkorn University

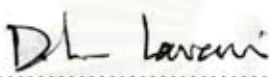
Thesis Title POROUS SILICON NITRIDE SYNTHESIS VIA THE
CARBOTHERMAL REDUCTION AND NITRIDATION OF
SILICA/RF GEL COMPOSITE

By Mr. Kanoksak Luyjew

Field of study Chemical Engineering

Thesis Advisor Assistant Professor Varong Pavarajarn, Ph.D.

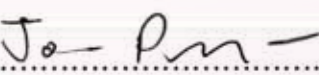
Accepted by the Faculty of Engineering, Chulalongkorn University in Partial
Fulfillment of the Requirements for the Master's Degree


..... Dean of the Faculty of Engineering
(Professor Direk Lavansiri, Ph.D.)

THESIS COMMITTEE


..... Chairman
(Associate Professor Tawatchai Charinpanitkul, Ph.D.)


..... Thesis Advisor
(Assistant Professor Varong Pavarajarn, Ph.D.)


..... Member
(Assistant Professor Joongjai Panpranot, Ph.D.)


..... Member
(Chanchana Thanachayanont, Ph.D.)

จุฬาลงกรณ์มหาวิทยาลัย

กนกศักดิ์ ลุ่มจิว : การสังเคราะห์ซิลิกอนไนไตรด์พูนด้วยกระบวนการคาร์โบเทอร์มอลรีดักชันและไนไตรเดชันของซิลิกา/อาร์เอฟเจลคอมพอสิต. (POROUS SILICON NITRIDE SYNTHESIS VIA THE CARBOTHERMAL REDUCTION AND NITRIDATION OF SILICA/RF GEL COMPOSITE.)

อ. ที่ปรึกษา : ผศ.ดร.วรงค์ ปวรจารย์, 81 หน้า.

การสังเคราะห์ซิลิกอนไนไตรด์พูนซึ่งเป็นวัสดุที่มีโครงสร้างเหมาะสมสำหรับใช้งานในการกรองภายใต้อุณหภูมิสูงจากซิลิกา/อาร์เอฟเจลคอมพอสิต ที่ถูกเตรียมด้วยวิธีโซล-เจลร่วมกับปฏิกิริยาโพลีเมอไรเซชันที่ใช้สารตั้งต้นของซิลิกาพร้อมด้วยได้ถูกศึกษา โดยพบว่า ซิลิกา/อาร์เอฟคาร์บอนคอมพอสิตจะถูกเปลี่ยนให้เป็นซิลิกอนไนไตรด์พูนด้วยกระบวนการคาร์โบเทอร์มอลรีดักชันและไนไตรเดชัน จากผลการทดลองพบว่า 3-อะมิโนโพรพิลไดรเมททอกซิไซเลน เป็นสารตั้งต้นของซิลิกาที่เหมาะสมในการทำปฏิกิริยาของการสังเคราะห์ซิลิกอนไนไตรด์พูน นอกจากนั้นยังพบว่าเวลาในการบ่มเจลไม่ส่งผลต่อความพูนของซิลิกอนไนไตรด์ การแลกเปลี่ยนน้ำด้วยที-บิวทานอลและอัตราส่วนเชิง โมลของซิลิกอนต่อคาร์บอนที่ใช้เป็นสารตั้งต้นในการเตรียมซิลิกาอาร์เอฟเจลเป็นปัจจัยหลักที่ส่งผลต่อความพูนของซิลิกอนไนไตรด์ ขณะที่เวลาในการทำปฏิกิริยาของปฏิกิริยาคาร์โบเทอร์มอลรีดักชันและไนไตรเดชันส่งผลต่อการรวมตัวและการซินเทอร์ของผลึกซิลิกอนไนไตรด์ที่เกิดขึ้น

สถาบันวิทยบริการ จุฬาลงกรณ์มหาวิทยาลัย

ภาควิชา.....วิศวกรรมเคมี..... ลายมือชื่อนิสิต..... กนกศักดิ์ ลุ่มจิว
สาขาวิชา.....วิศวกรรมเคมี..... ลายมือชื่ออาจารย์ที่ปรึกษา.....
ปีการศึกษา.....2549.....

4870202821 : MAJOR CHEMICAL ENGINEERING
 KEY WORD: POROUS / SILICON NITRIDE / RF GEL / CARBOTHERMAL
 REDUCTION / NITRIDATION

KANOCSAK LUYJEW: POROUS SILICON NITRIDE SYNTHESIS VIA
 THE CARBOTHERMAL REDUCTION AND NITRIDATION OF
 SILICA/RF GEL COMPOSITE. THESIS ADVISOR: ASST. PROF.
 VARONG PAVARAJARN, Ph.D., 81 pp.

The synthesis of porous silicon nitride, one of the most promising structural materials for filter at high-temperature applications, from silica/ RF gel composite which was prepared by combining sol-gel and polymerization methods with the use of silica, precursor was investigated. Silica/RF carbon composite was converted into porous silicon nitride via the carbothermal reduction and nitridation. From the results, 3-Amino propyl trimethoxysilane was found to be a suitable silica precursor for the synthesis of porous silicon nitride. It was also found that aging time of silica/RF gel does not affect the porosity of silicon nitride. Solvent exchange with *t*-butanol and molar ratio of silicon and carbon that are used in the preparation of silica/RF gel are the major factor affecting in the porosity of silicon nitride. The reaction time for the carbothermal reduction and nitridation is an important factor affecting the agglomeration and sintering of silicon nitride particles.

สถาบันวิทยบริการ
 จุฬาลงกรณ์มหาวิทยาลัย

Department.....Chemical Engineering.....Student's signature.....*Kanoksak Luyjew*
 Field of study...Chemical Engineering....Advisor's signature.....*Varong Pavrajarn*
 Academic year2006.....

ACKNOWLEDGEMENTS

The author would like to express his greatest gratitude to his advisor, Assistant Professor Varong Pavarajarn, for his help, invaluable suggestions and guidance throughout the entire of this work. His precious teaching the way to be good in study and research has always been greatly appreciated. In addition, his friendliness motivated the author with strength and happiness to do this work.

The author wishes to express his thanks to Associate Professor Tawatchai Charinpanitkul who has been the chairman of the committee for this thesis, as well as Dr. Chanchana Thanachayanont and Assistant Professor Joongjai Panpranot, who have been his committee members. He would also like to register his thanks to Nattaporn Tonanon, for a number of suggestions and kindness understanding and Mr. Adisak siyasukh, for their help during his study. In addition, the many others, not specifically named, in Center of Excellence on Catalysis and Catalytic Reaction Engineering, Department of Chemical Engineering, who have provided his with encouragement and co-operate along this study, please be ensured that he thinks of you.

Moreover, the author would like to thank the department of Chemical Engineering, as well as the Graduate School of Chulalongkorn University for their financial support and National Metal and Materials Technology Center (MTEC) for Transmission Electron Microscope analysis fee discount. Finally, he would like to dedicate the achievement of this work to his dearest parents. Their unyielding support and unconditional love have always been in his mind.

CONTENTS

	Page
ABSTRACT (IN THAI)	iv
ABSTRACT (IN ENGLISH).....	v
ACKNOWLEDGEMENTS.....	vi
CONTENTS.....	vii
LIST OF TABLES.....	ix
LIST OF FIGURES.....	xi
CHAPTER	
I INTRODUCTION.....	1
II THEORY AND LITERATURE SURVEY.....	4
2.1 Silicon Nitride Powder.....	4
2.2 Crystal Structure of Silicon Nitride.....	5
2.3 Carbothermal Reduction and Nitridation of Silica.....	6
2.4 Fabrication of Porous Silicon Nitride Ceramics	7
2.5 Sol-Gel Processing.....	10
2.6 Resorcinol–Formaldehyde (RF) Gel.....	11
2.7 Mechanisms for Crystal Growth from Gas Phase.....	13
III EXPERIMENTAL.....	15
3.1 Materials.....	15
3.2 Preparation of Silica/RF Hydrogel.....	15
3.3 Preparation of Porous Silica/Carbon Composite.....	16
3.4 Carbothermal Reduction and Nitridation	16
3.5 Characterization of the Products.....	18
3.5.1 X-ray Diffraction Analysis (XRD).....	18
3.5.2 Fourier-Transform Infrared Spectroscopy (FT-IR).....	18
3.5.3 Thermogravimetric Analysis (TGA).....	18
3.5.4 Scanning Electron Microscopy (SEM).....	19
3.5.5 Transmission Electron Microscope (TEM).....	19
3.5.6 Surface Area Measurement.....	19
3.5.7 Gas Chromatography.....	19

	Page
IV RESULTS AND DISCUSSION.....	21
4.1 Preliminary Experiments.....	21
4.2 Effect of Silica Precursor.....	27
4.3 Effect of Si-to-C Ratio on Properties of Silicon Nitride.....	30
4.4 Effect of Solvent Exchange on Properties of Silicon Nitride...	35
4.5 Effect of Aging Time on Properties of Silicon Nitride.....	41
4.6 Effect of pH on Properties of Silicon Nitride.....	44
4.7 Effect of Reaction Time on Properties of Silicon Nitride.....	50
V CONCLUSIONS AND RECOMMENDATIONS.....	58
5.1 Conclusions.....	58
5.2 Recommendations for Future Work.....	59
REFERENCES.....	60
APPENDICES.....	65
APPENDIX A Calculation of molar ratio of silicon and carbon in RF gel composite.....	66
APPENDIX B Data of pore diameter and pore volume.....	68
APPENDIX C Calibration curves for quantitative analysis by gas chromatography.....	73
APPENDIX D Pictures of silica/RF composites.....	75
APPENDIX E SEM micrographs of silicon nitride powder synthesized after calcination process.....	76
APPENDIX F List of publication.....	78
VITA.....	81

LIST OF TABLES

Table	Page
2.1 Typical properties of silicon nitride powders produced by various processing techniques.....	5
3.1 Operating conditions for gas chromatograph.....	20
4.1 Surface area of silicon nitride powder synthesized with various Si/C molar ratios after calcination.....	32
4.2 Surface area of silicon nitride powder synthesized after calcination with various aging times.....	43
4.3 Surface area of calcined silicon nitride powder with Si/C ratio of 0.05, synthesized with various pH values, compared with RF carbon.....	47
4.4 Sample mass loss after nitridation at various reaction times.....	52
B1 Data of pore diameter and pore volume of calcined sample with molar ratio of Si/C = 0.05, synthesized with solvent exchange and no aging.....	68
B2 Data of pore diameter and pore volume of calcined sample with molar ratio of Si/C = 0.05, synthesized with solvent exchange and aged for 1 day.....	68
B3 Data of pore diameter and pore volume of calcined sample with molar ratio of Si/C = 0.05, synthesized with solvent exchange and aged for 3 days.....	69
B4 Data of pore diameter and pore volume of calcined sample with molar ratio of Si/C = 0.05, synthesized with solvent exchange and aged for 5 days.....	69
B5 Data of pore diameter and pore volume of calcined sample with molar ratio of Si/C = 0.05, synthesized with solvent exchange and aged for 7 days.....	70
B6 Data of pore diameter and pore volume of calcined sample with molar ratio of Si/C = 0.07, synthesized with solvent exchange and no aging.....	70

Table	Page
B7 Data of pore diameter and pore volume of calcined sample with molar ratio of Si/C = 0.07, synthesized with solvent exchange and aged for 1 day.....	71
B8 Data of pore diameter and pore volume of calcined sample with molar ratio of Si/C = 0.07, synthesized with solvent exchange and aged for 3 days.....	71
B9 Data of pore diameter and pore volume of calcined sample with molar ratio of Si/C = 0.07, synthesized with solvent exchange and aged for 5 days.....	72
B10 Data of pore diameter and pore volume of calcined sample with molar ratio of Si/C = 0.07, synthesized with solvent exchange and aged for 7 days.....	72

LIST OF FIGURES

Figure	Page
2.1 β -Si ₃ N ₄ unit cell.....	6
2.2 α - Si ₃ N ₄ unit cell.....	6
2.3 Reaction mechanism of the sol-gel polymerization of resorcinol with formaldehyde.....	12
2.4 Mechanism of two types of gas phase process.....	14
3.1 Schematic diagram of the tubular flow reactor system.....	17
4.1 XRD patterns of nitrated powders obtained by using: (a) pure RF carbon gel (b) RF carbon gel with APTMS.....	21
4.2 SEM micrographs of RF carbon gel before and after nitridation.....	22
4.3 SEM micrographs of silica/RF composite with the Si/C ratio of 0.07.....	23
4.4 TGA analysis in nitrogen atmosphere of silica/RF gel at various molar ratios of silicon and carbon.....	25
4.5 TGA analysis in oxygen atmosphere of pyrolyzed silica/RF gel at various molar ratios of silicon and carbon.....	25
4.6 TEM micrographs of the nitrated product with molar ratio of Si/C = 0.05.....	26
4.7 XRD patterns of nitrated powders obtained after calcinations at 700°C for 10 h used various kinds of silica precursor	28
4.8 FT-IR spectra of silica/RF composite	29
4.9 FT-IR spectra of silica precursor used in the preparation of silica/RF composite.....	29
4.10 FT-IR spectra of silica/carbon composite at various molar ratios of Si/C.....	30
4.11 XRD patterns of silicon nitride powder synthesized with various Si/C molar ratios, after calcinations at 700°C for 10 h.....	32
4.12 SEM micrographs of the silicon nitride synthesized with various Si/C molar ratios, after calcinations.....	33

Figure	Page
4.13 TGA analysis of the final products after calcination process with various molar ratios of silicon- to-carbon.....	34
4.14 SEM micrographs of silica/RF composite with Si/C ratio of 0.07, before pyrolysis.....	36
4.15 SEM micrographs of the silicon nitride powder with Si/C ratio of 0.07, after calcined.....	36
4.16 TEM micrographs and SAED patterns of the silicon nitride powder synthesized with Si/C molar ratio = 0.05 without solvent exchange, after calcinations process.....	37
4.17 TEM micrographs and SAED patterns of the silicon nitride powder synthesized with Si/C molar ratio = 0.05 with solvent exchange, after calcinations process.....	38
4.18 TEM micrographs and SAED patterns of the silicon nitride powder synthesized with Si/C molar ratio = 0.07 without solvent exchange, after calcinations process.....	39
4.19 TEM micrographs and SAED patterns of the silicon nitride powder synthesized with Si/C molar ratio = 0.07 with solvent exchange, after calcinations process.....	39
4.20 Pore size distribution of calcined silicon nitride powder prepared from silica/RF composite with Si/C ratio of 0.05, using various aging times.....	41
4.21 Pore size distribution of calcined silicon nitride powder prepared from silica/RF composite with Si/C ratio of 0.07, using various aging times.....	42
4.22 The average pore diameters of silicon nitride synthesized with various aging times.....	42
4.23 Pore size distribution of the calcined silicon nitride powders, which were synthesized from silica/RF composite prepared at different pH value....	45
4.24 XRD patterns of the calcined silicon nitride powders prepared from silica/RF solution at different pH values.....	46

Figure	Page
4.25 TEM micrograph and SAED pattern of the silicon nitride powder synthesized with Si/C molar ratio = 0.05 at pH 3.0, after calcination process.....	48
4.26 TEM micrograph and SAED pattern of the silicon nitride powder synthesized with Si/C molar ratio = 0.05 at pH 4.0, after calcination process.....	48
4.27 TEM micrographs and SAED patterns of the silicon nitride powder synthesized with Si/C molar ratio = 0.05 at pH 5.0, after calcination process.....	49
4.28 XRD patterns of products from the carbothermal reduction and nitridation of silica/RF composite at molar ratio Si/C=0.05 with various reaction times.....	50
4.29 XRD patterns of products from the carbothermal reduction and nitridation of silica/RF composite at molar ratio Si/C=0.07 with various reaction times.....	51
4.30 Concentration of carbon monoxide gas which was generated during the carbothermal reduction and nitridation.....	52
4.31 TEM micrographs and SAED pattern of the silicon nitride powder with Si/C molar ratio = 0.05 synthesized via the carbothermal reduction and nitridation for 8 h, after calcination process.....	54
4.32 TEM micrographs and SAED pattern of the silicon nitride powder with Si/C molar ratio = 0.05 synthesized via the carbothermal reduction and nitridation for 10 h, after calcination process.....	55
4.33 TEM micrograph and SAED pattern of the silicon nitride powder with Si/C molar ratio = 0.07 synthesized via the carbothermal reduction and nitridation for 8 h, after calcination process.....	56
4.34 TEM micrograph and SAED pattern of the silicon nitride powder with Si/C molar ratio = 0.07 synthesized via the carbothermal reduction and nitridation for 10 h, after calcination process.....	57

Figure	Page
C1 The calibration curve for hydrogen	73
C2 The calibration curve for carbon monoxide.....	74
C3 The calibration curve for nitrogen.....	74
D1 Silica/RF composite obtained after pyrolysis process.....	75
D2 Silica/RF composite obtained after the carbothermal reduction and nitridation.....	75
E1 SEM micrograph of silicon nitride powder with Si/C molar ratio of 0.02 prepared without solvent exchange after calcination process.....	76
E2 SEM micrograph of silicon nitride powder with Si/C molar ratio of 0.07 prepared without solvent exchange after calcination process.....	76
E3 SEM micrograph of silicon nitride powder with Si/C molar ratio of 0.07 prepared without solvent exchange after calcination process.....	77
E4 SEM micrograph of silicon nitride powder with Si/C molar ratio of 0.07 prepared with solvent exchange after calcination process.....	77

CHAPTER I

INTRODUCTION

Silicon nitride (Si_3N_4) is one of the most promising structural materials for high-temperature and high mechanical stress applications. It was developed in the 1960s in a search for fully dense, high-strength and high-toughness materials. Silicon nitride has better high-temperature capabilities than most metals. In addition, its low thermal expansion coefficient gives good thermal shock resistance compared with most ceramic materials.

Porous ceramics are essential for many industries, where high surface area and insulating character are required. They can be used as filters in diesel engine, filters for exhausted emission, filters for molten metals, membrane reactors, and catalyst carriers (Zhang et al. 2005). Mesoporous silicon nitride has been suggested as a good candidate for base-catalysed reactions. Potassium-loaded high surface area silicon nitride was also found to be an efficient superbase catalyst suitable for alkene isomerisation reactions (Kaskel and Schlichte 2001). Porosity in ceramic also reduces density of specimen. With the expansion of applications for porous ceramics, high porosity as well as high strength are required at the same time.

Porous ceramics have also been attracting great interest for various applications relating to separation in severe environments, in which other materials such as metals or organic materials cannot be used. Porous ceramic thin films with fine pores are candidate materials for the separation of specific gas, liquid and solid phases under high temperature or high corrosive environments.

Many researches have been done on the preparation of porous silicon nitride and silicon nitride-based composites. Porous silicon nitride ceramics with a fibrous microstructure have been synthesized directly by carbothermal nitridation of silica, in which carbon black was used as carbon source and $\alpha\text{-Si}_3\text{N}_4$ was used as seed

(Yang et al. 2005a). In the early works, porous silicon nitride ceramics with high porosity have been fabricated by adding small amount of carbon (0.7–3.4 wt %) into α - Si_3N_4 powder before sintering. Then, porous $\text{SiC}/\text{Si}_3\text{N}_4$ nanocomposite ceramics have also been synthesized using the same approach, but using different ratio of $\text{C}/\text{Si}_3\text{N}_4$.

Silicon nitride can be prepared by the carbothermal reduction and nitridation of silica/carbon mixture. This process is the earliest method used for Si_3N_4 production. The process involves the reaction of carbon and silica in a flowing nitrogen atmosphere at temperatures in the range from 1200° up to 1450°C .

RF gel was prepared by resorcinol (R) and formaldehyde (F) according to the method of Pekala. Porous carbon gels were obtained from drying and carbonization of RF gel that have high specific surface area. Thus, the porous silica/carbon composite could be formed by combining co-polymerization and sol-gel processes using resorcinol and formaldehyde as sources for porous carbon matrix and a precursor for silica.

In this research, porous silicon nitride is synthesized by the carbothermal reduction and nitridation of the silica/carbon composite, whereas the composite is formed by carbonization of dried gel prepared via sol-gel process using resorcinol (R), formaldehyde (F) and silicon-containing species as precursors. The composite fabricated by such approach has been proved to have mesoporous structure with high specific surface area. Effects of various factors, such as type of silica precursor, molar ratio of Si and C, aging time, solvent exchange and conditions for the carbothermal reduction and nitridation, on the structure of silicon nitride are investigated in this work. The scopes of this study are as following:

1. Porous silicon nitride is synthesized by the carbothermal reduction and nitridation of silica/carbon composite, which is prepared by sol-gel method.
2. Parameters of the investigated reaction are divided into two parts, i.e. preparation of silica/carbon composite and conversion of the silica/carbon composite into porous silicon nitride.
 - In term of silica/carbon composite preparation, the investigated parameters include type of silica precursor, the molar ratio of silica and carbon, aging time and method to remove solvent from the obtained gel.
 - In term of converting silica/carbon composite into porous silicon nitride, the main investigated parameter is reaction time to observe the progress of the reaction.

This thesis is divided into five parts. The first three parts describe general information about the study, while the following two parts emphasize on the results and discussion from the present study. The background and scope of the study are presented in Chapter I. Chapter II consists of the theory and literature survey, while the experimental systems and procedures used in this study are shown in Chapter III. The experimental results, including an expanded discussion, are given in Chapter IV. Finally, in the last chapter, the overall conclusion from the results and some recommendations for future work are presented.

CHAPTER II

THEORY AND LITERATURE SURVEY

2.1 Silicon Nitride Powder

Silicon nitride is a high-temperature structural ceramic that does not exist in nature. It is not easy to obtain high purity silicon nitride powder with fine grain size, narrow size distribution and economically. The following techniques are usually applied to synthesize α -Si₃N₄ powders (Yang et al. 2005a): (1) nitridation of metallic silicon powder, (2) gas-phase reaction of silane, (3) carbothermal reduction of silica in nitrogen atmosphere, and (4) precipitation and thermal decomposition of silicon diimide. For industrial production of silicon nitride powder, silicon, silica and silicon tetrachloride (SiCl₄) are the three commonly used starting materials for the aforementioned processes, because they are available in high purity on an economic basis or can be easily purified. Typical properties of silicon nitride powder produced via these processes are shown in Table 2.1.

สถาบันวิทยบริการ
จุฬาลงกรณ์มหาวิทยาลัย

Table 2.1 Typical properties of silicon nitride powders produced by various processing techniques (Matovic 2003).

	Direct nitridation of silicon	Vapor phase synthesis	Carbothermal nitridation	Diimide synthesis
Specific surface area (m ² /g)	8-25	3.7	4.8	10
Oxygen content (wt %)	1.0-2.0	1	1.6	1.4
Carbon content (wt %)	0.1-0.4	-	0.9-1.1	0.1
Metallic impurities (wt %) Σ Fe, Al, Ca	0.07-0.15	0.03	0.06	0.005
Crystallinity (%)	100	60	100	100
α/(α+β) (%)	95	95	95	85

2.2 Crystal Structure of Silicon Nitride

It has been generally accepted that there are two forms of crystalline silicon nitride, designated as α and β forms. Detailed X-ray diffractometry (XRD) examinations in the mid-1950s have proved that the crystal structure of both α and β polymorphs are hexagonal (Turkdogan et al. 1958). However, their respective structural dimensions are different. The structures of β -phase and α -phase are shown in Figure 2.1 and Figure 2.2 respectively.

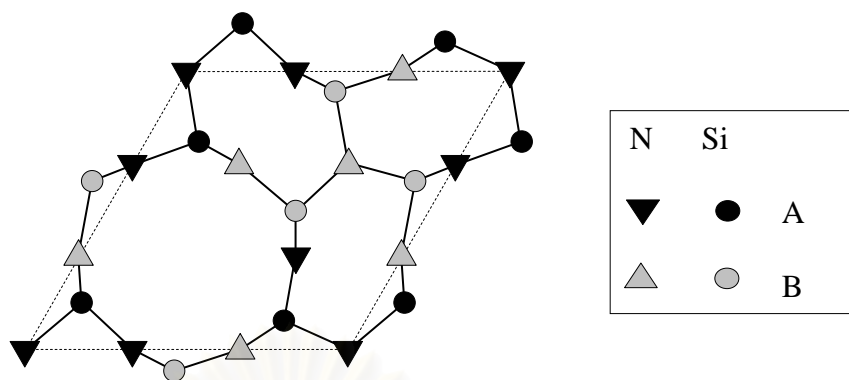


Figure 2.1 β - Si_3N_4 unit cell: the structure of β - Si_3N_4 can be described as a stacking of Si-N layers in ...ABAB... sequence.

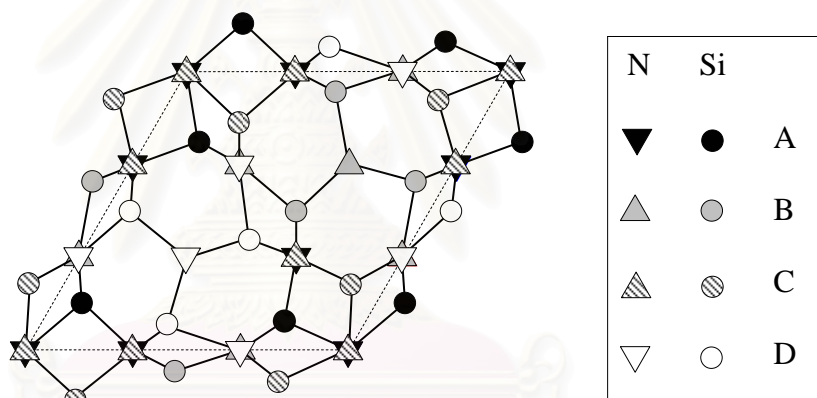


Figure 2.2 α - Si_3N_4 unit cell: the structure of α - Si_3N_4 can be described as a stacking of Si-N layers in ...ABCDABCD... sequence.

2.3 Carbothermal Reduction and Nitridation of Silica

The carbothermal reduction of silica powder under nitrogen is the earliest method used for silicon nitride production (Riley 2000). The process can be described by the following overall reaction (Segal 1985).



Fine α -silicon nitride powder can be produced directly by using very fine silica. The reaction is usually performed at temperature in the range of 1200-1450°C, depending on the reactivity of raw materials. Nevertheless, the overall reaction is reported to be slow, requiring many hours to complete. Since the reaction relies on solid contacts between silica and carbon, excess amount of carbon is required for full transformation of silica to silicon nitride, which often results in free carbon remaining in the nitrated powder. By annealing this powder in air, the residual carbon can be oxidized, but so is the silicon nitride. Consequently, the product powder produced by this method often suffers from purity problem associated with residual carbon and oxygen content. However, this route has an advantage in availability of the reactants, i.e. C and SiO₂. The characteristics of the Si₃N₄ powder resulting from the carbothermal reduction process depend on many factors namely the C/SiO₂ ratio, the nitrogen flow rate, reaction temperature, particle size and specific surface area of silica and carbon as well as the presence of impurities.

2.4 Fabrication of Porous Silicon Nitride Ceramics

Pure silicon nitride is difficult to produce as a fully dense specimen. This covalently bonded material is not readily sinterable and cannot be heated over 1850°C, as it dissociates into silicon and nitrogen. Dense silicon nitride can only be made using techniques that give bonding indirectly, e.g. an addition of small amount of chemicals to aid densification. These chemicals are known as sintering aids, which commonly induce a degree of liquid phase sintering.

Up until now, porous Si₃N₄ has been successfully prepared by partial sintering (Kawai et al. 1997; Yang et al. 2003), restrained sintering (Yang et al. 2001), type casting (Inagaki et al. 2000), partial hot-pressing (Yang et al. 2002), partial forge sintering (Yang et al. 2005a), addition of fugitive inclusions (Díaz et al. 2005; Yang et al. 2005b), or non-oxidation process (Kaskel and Schlichte 2001). Most of these

processes requires α - Si_3N_4 as the starting powder. Consequently, the components fabricated from these processes are too costly for many applications, because Si_3N_4 powder is expensive and high-temperature sintering is required (Yang et al. 2005a).

(1) Partial sintering

Partial sintering is a process that has been developed from the conventional sintering for powder compact. It is generally used to fabricate porous ceramic materials composed of oxides (Yang et al. 2003). In this process, porous silicon nitride ceramic can be prepared by varying the ratio of the densification additives or by changing the sintering temperature (Díaz et al. 2005). Sintering additives used are usually Al_2O_3 , Y_2O_3 or Yb_2O_3 . Densification (porosity) is controlled by adjusting the additives and the sintering process.

The densification of Si_3N_4 with Y_2O_3 - Al_2O_3 or Yb_2O_3 - Al_2O_3 sintering additives starts at 1400–1500°C, whereas >90% relative density can be achieved for a sample with high additive content (Suttor and Fischman 1992; Yang et al. 2000). The additives react with the native SiO_2 on the surface of Si_3N_4 grains to produce a glass or crystalline phase.

(2) Partial hot-pressing

This method employs high temperature and high pressure in sintering process. Partial hot-pressing (PHP) using Yb_2O_3 as the sintering additive and α -silicon nitride is a starting powder to prepared porous silicon nitride materials. In this method, the precise porosity can be controlled. The powders were weighed and packed into the hot-pressing mold. In the mold densification occurred with the increasing temperature and pressure. Thus, the density can be simply and precisely determined by the configuration of mold and the amount of starting power. The PHP was carried out in a furnace at a temperature of 1800°C under nitrogen atmosphere. A gas pressure of 30 MPa was applied at temperature higher than 1100°C (Yang et al. 2002).

(3) Partial forge sintering

The partial sinter-forging is a very simple technique, which does not require only conventional hot-pressing equipment and graphite dies. In this technique, microstructure and porosity can be controlled by choosing suitable sintering temperature, time and mechanical press. Partial sinter-forging was conducted using a hot-press furnace with mechanical press was applied at high temperature.

Porous silicon nitrides with aligned rod-like grains were fabricated by using partial sinter-forging technique, where uniaxial pressure was applied after soaking at elevated temperatures (Kondo et al. 2002). Rod-like silicon nitride grains were formed during the soaking, and the grains were aligned by the subsequent forging. The grains were aligned perpendicularly to the pressing direction. The microstructure also shows protruding rod-like grains as well as holes or hollows.

(4) Addition of fugitive inclusions

Porous silicon nitride can also be fabricated by using a removable fugitive particle during the sintering process. The pore size in the sintered silicon nitride depends upon the size of the fugitive particle (Yang et al. 2002). The porous Si_3N_4 ceramics fabricated by this process has large regularly-spaced pores, good permeability and has been used for filtration applications. In this method, fugitive particles are added into an initial ceramic mixture. These particles can be divided into: (i) equiaxial organic particles, such as starch powder (Díaz and Hampshire 2004), plastic particles (carbohydrate powders) (Lyckfeldt and Ferreira 1998), and (Yang et al.) long fibers, such as cotton threads (Liu 1997) and metal wires (Zhang et al. 2001). The mixed powder is obtained, following by drying and sintering in furnace at 1800°C under flowing of nitrogen. Excellent permeability is achievable for porous ceramics with unidirectional pore because gas can flow directly through the pore. However, the fabrication process is too complicated and difficult for large components. Short fibers can also be used as a pore-forming agent. The resultant pores are random, but the pore

morphology is a long, rod-shaped tunnel, which contributes to high permeability (Yang et al. 2005b).

(5) Non-oxidation sol-gel process

In this method, the process is operated under an anhydrous nitrogen atmosphere or in an argon-filled glove box. Silicon diimide gel was prepared by an acid-catalyzed ammonolysis of tris(dimethylamino)silylamine (Cheng et al. 2004). The obtained gel was pyrolyzed under ammonia flow leading to the formation of amorphous silicon nitride. Kaskel et al. (2001) prepared silicon imido nitride by ammonolysis of silicon tetrachloride in organic solvents followed by removal of ammonium chloride in ammonia atmosphere at elevated temperature. The obtained silicon nitride in this method exhibited a mesoporous structure with a high surface area, narrow pore-size distribution and no carbon contamination. Although this technique can result in porous silicon nitride with high surface area, the process is complicated since it is highly sensitive to oxygen.

2.5 Sol-Gel Processing

Sol-gel process is a versatile solution process for the synthesis of advanced materials, including ceramics and organic-inorganic hybrids. In general, the sol-gel process involves transition of a solution system from colloidal liquid "sol" into solid "gel" phase. Utilizing the sol-gel process, it is possible to fabricate advanced materials in a wide variety of forms, e.g. ultrafine or spherical shaped powders, thin film coatings, fibers, porous or dense materials, and extremely porous aerogel materials.

The starting materials used in the preparation of the "sol" are usually inorganic metal salts or metal organic compounds such as metal alkoxides. In a typical sol-gel process, the precursor is subjected to a series of hydrolysis and polymerization reactions to form a colloidal suspension, or "sol". Further processing of the "sol" makes it possible to make materials in different forms.

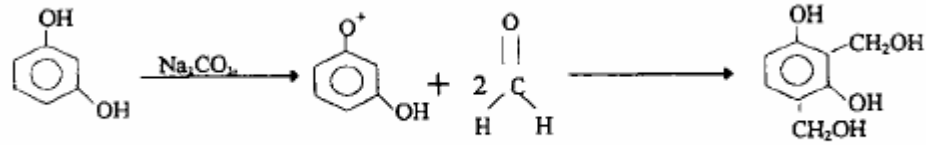
2.6 Resorcinol–Formaldehyde (RF) Gel

RF gel was first synthesized by Pekala via sol–gel polycondensation of resorcinol (R) and formaldehyde (F) with sodium carbonate (C) as catalyst (Tonanon et al. 2005). A polycondensation reaction between resorcinol and formaldehyde results in a three-dimensional polymer matrix called the RF hydrogel. Then, mesoporous carbon gel (CG), which is consisted of solid carbon skeleton can be formed by heat treatment of the RF gel after solvent exchange and drying (Lin and Ritter 1997; Pekala 1989).

The major reactions between resorcinol and formaldehyde include (1) an addition reaction to form hydroxymethyl derivatives ($-\text{CH}_2\text{OH}$) of resorcinol, and (2) a condensation reaction of the hydroxymethyl derivatives to form methylene ($-\text{CH}_2-$) and methylene ether ($-\text{CH}_2\text{OCH}_2-$) bridged compounds (Lin and Ritter 1997). Figure 2.3 illustrates a brief mechanism of the sol-gel polymerization of resorcinol with formaldehyde.

For the formation of carbon gel, pH of the solution during RF gel synthesis is one of the most crucial factor affecting properties of the resulting carbon gel. The initial pH of RF solution has effects on surface area, pore volume, pore size distribution and nanostructure of the gel. A lower initial pH yields carbon gel with higher surface area and pore volume. If the initial pH is too high, the condensation reaction is hindered, resulting in a less cross-linked RF structure that would collapse during drying and pyrolysis and leading to carbon gel with lower surface area and pore volume (J. Aguado-Serrano et al. 2004; Lin and Ritter 1997).

1. Addition Reaction



2. Condensation Reaction

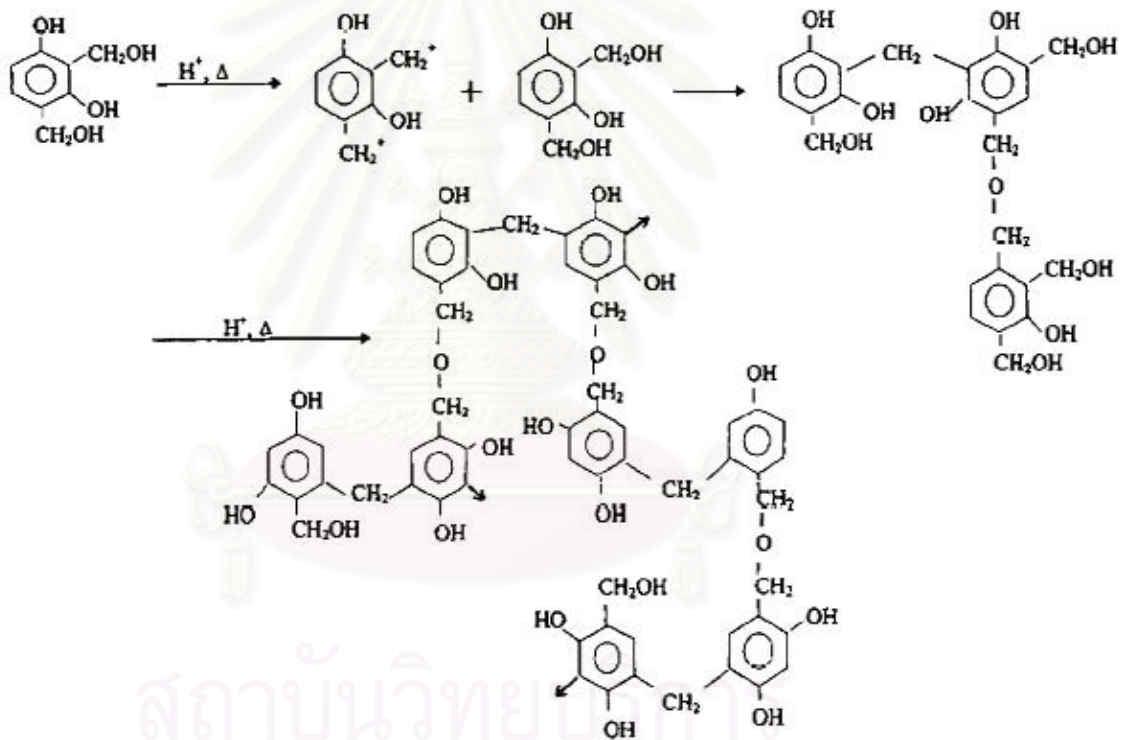


Figure 2.3 Reaction mechanism of the sol-gel polymerization of resorcinol with formaldehyde.

Pore structure and surface area of the final carbon gel depend not only on the conditions of RF gel synthesis, but also on the drying and carbonizing techniques. Three kinds of drying techniques are available to convert the hydrogel to a solid RF gel. The first method is drying in an inert atmosphere, which gives a RF xerogel (Pekala 1989). A second method is freeze-drying, which yields a RF cryogel (Tamon et al. 1999). The third method employs supercritical extraction with carbon dioxide, which results in a RF aerogel (Lin and Ritter 1997).

The method of drying RF gels influences the structure of carbon gels. Xerogels, obtained by heating the RF hydrogel in an inert atmosphere, have the most compact structure with the lowest specific surface area ($<900 \text{ m}^2/\text{g}$). The highest surface area is found in the gel lyophilized after freeze-drying in *t*-butanol ($>2500 \text{ m}^2/\text{g}$), but the resulting carbon cryogel is not structurally stable, i.e. the measured surface area decreasing with time. Supercritical extraction with liquid carbon dioxide yields aerogels with an intermediate value for the surface area (ca. $1000 \text{ m}^2/\text{g}$) (Czakkal et al. 2005).

2.7 Mechanisms for Crystal Growth from Gas Phase

Two types of mechanism are often used to explain the crystal growth associated with gas phase, as shown in Figure 2.4 (Kawai and Yamakawa 1998). In the vapor-solid (VS) mechanism, Figure 2.4(a), chemical species diffuse toward a substrate through an interfacial gas layer, and adsorbed on the surface of the substrate. The adsorbed species may be mobile on the surface. Subsequently, nucleation and crystal growth occur, accompanied by the elimination of any by-product. In VS mechanism, the diffusion of the chemical species in the gas phase and their surface migration on the substrate are fast. Therefore, high deposition rate will be obtained if a reaction between the chemical species is fast enough. On the other hand, there are few studies focusing on the use of the vapor-liquid-solid (VLS) mechanism. As shown in Figure 2.4(b), if liquid-phase exists on a substrate, chemical species must be first dissolved in the liquid phase for crystal growth. Next, they diffuse in liquid and

adsorbed on the substrate. Finally, crystal growth occurs via nucleation in the liquid phase. The diffusion rate of the chemical species in the liquid phase is probably much slower than in gas phase. Therefore, the rate of the supplement of chemical species to nucleus for crystal growth is very small. This results in high nucleation density and the formation of the finer crystals than those through the VS mechanism.

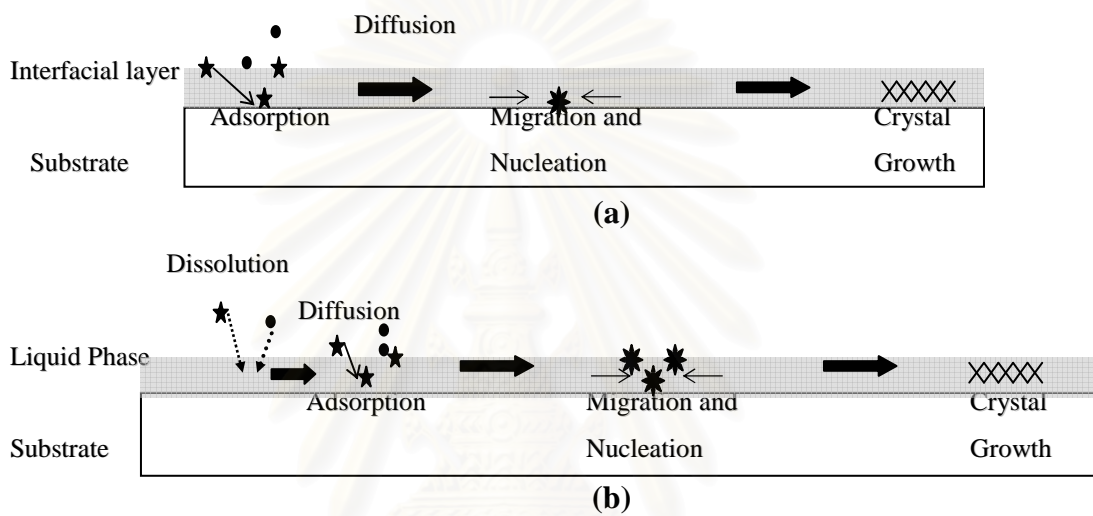


Figure 2.4 Mechanism of two types of gas phase process: (a) VS mechanism, (b) VLS mechanism.

CHAPTER III

EXPERIMENTAL

This chapter describes the experimental systems and procedures used in this study. The chapter is divided into five sections. Section 3.1 is raw materials. Section 3.2 is the preparation of silica/RF hydrogel. Section 3.3 and 3.4 present preparation of porous silica/carbon composite and porous silicon nitride, respectively. Characterization of the products is presented in the last section.

3.1 Materials

Chemicals used in this study include 3-amino propyl trimethoxysilane (APTMS), tetraethyl orthosilicate (TEOS), resorcinol (R), formaldehyde (F) solution sodium carbonate anhydrous, sodium silicate solution and nitric acid (HNO_3).

3-Amino propyl trimethoxysilane (APTMS) 97% and tetraethyl orthosilicate (TEOS) 98% were purchased from Sigma-Aldrich Chemical Company and used as received.

Resorcinol 99%, formaldehyde solution 37%, sodium carbonate anhydrous and nitric acid were purchased from Asia Pacific Specialty Chemicals Limited and used as received.

Sodium silicate solution extra pure was purchased from Merck Chemicals Limited and used as received.

3.2 Preparation of Silica/RF Hydrogel

The synthesis of silica/RF gel was carried out by co-polymerization and sol-gel processes using resorcinol, formaldehyde, sodium carbonate and distilled water as raw materials for RF gel structure and APTMS as a precursor for silicon. 9 g resorcinol and 0.0106 g sodium carbonate were dissolved in 10 ml distilled water. After homogenizing, 12.6 ml formaldehyde was added. The solution was stirred at room temperature for 15 min. Then, APTMS in the predetermined amount was added

to the solution with continuous stirring. The silica/RF gel was aged for the predetermined period of time at room temperature without stirring. After aging, solvent in the gel was removed by solvent process, i.e. the sample was immersed in 50 ml of *t*-butanol for 24 h, renewed with fresh *t*-butanol everyday. The solvent exchange process was repeated for three times. Finally, silica/RF gel was removed from *t*-butanol and dried in oven at 110°C for 16 h to obtain silica/RF hydrogel.

In case of pH control, the pH of the solution was adjusted to desired value by adding 10% HNO₃ to the solution after formaldehyde was added.

3.3 Preparation of Porous Silica/Carbon Composite

Porous silica/carbon composite was obtained by pyrolysis of the dried silica/RF hydrogel in the step-wised fashion from 250 to 750°C. Pyrolysis was conducted under a 200 ml/min flow of nitrogen gas in a tubular flow reactor. At first, the silica/RF hydrogel was heated to 250°C at a constant heating rate of 10°C /min, and kept at this temperature for 2 h. Then it was heated to 750°C at a constant heating rate of 10°C /min and kept at this temperature for 4 h. The product from this step is silica/carbon composite.

3.4 Carbothermal Reduction and Nitridation

For the carbothermal reduction and nitridation the silica carbon composite powder was put into an alumina tray (25 mm x15 mm x 5 mm deep) and placed in the horizontal tubular flow reactor. The schematic diagram of the reactor system is shown in Figure 3.1. The powder was then heated in continuous flow of argon at 50 l/h to 1450°C, at the rate of 10°C/min. After the system had reached the desired temperature, the argon stream was replaced with a mixture of 90% nitrogen and 10% hydrogen with total flow rate at 50 l/h. The reaction was kept in this condition for 6 h.

The obtained product was later calcined in calcine box at 700°C for 10 h to remove the excess carbon.

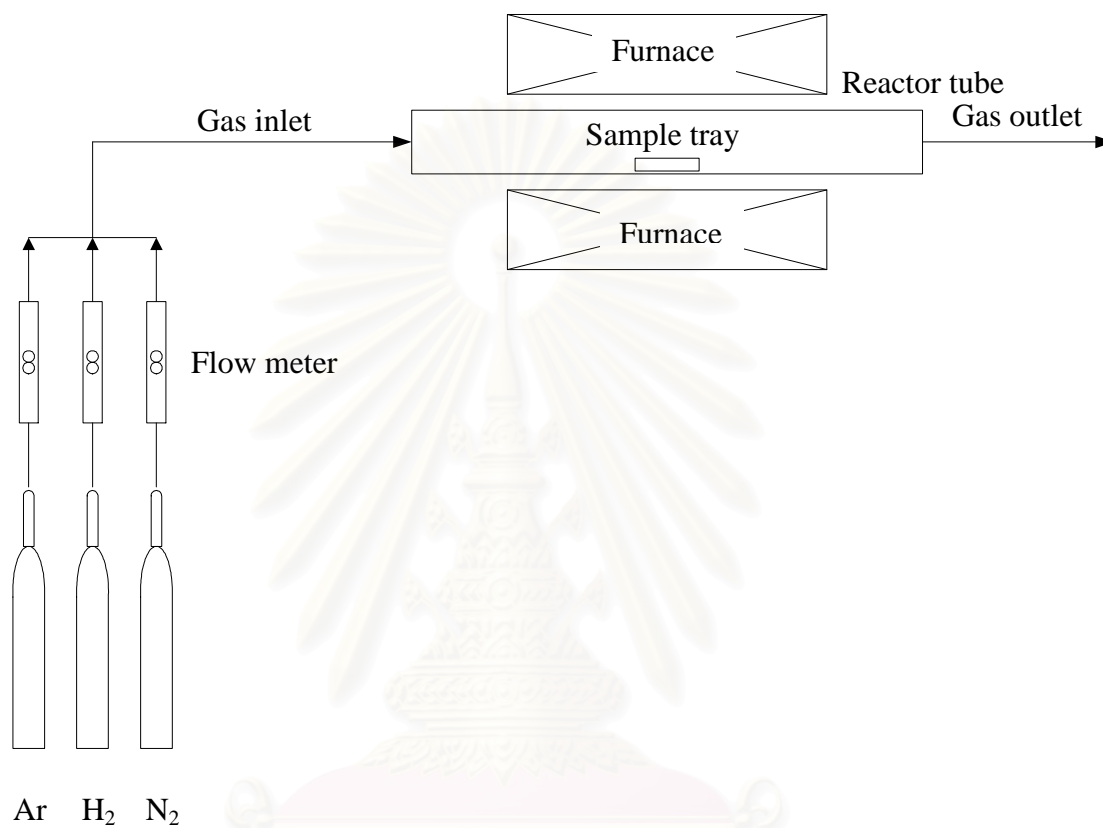


Figure 3.1 Schematic diagram of the tubular flow reactor system.

สถาบันวิทยบริการ
จุฬาลงกรณ์มหาวิทยาลัย

3.5 Characterization of the Products

The obtained products were characterized by using various techniques, as following:

3.5.1 X-ray Diffraction Analysis (XRD)

Crystalline phases of the product were determined from X-ray diffraction analysis, using a SIEMENS D5000 diffractometer with CuK α radiation. Each sample was scanned in the range of $2\theta = 10-50^\circ$ with a step size of $2\theta = 0.02^\circ$.

3.5.2 Fourier-Transform Infrared Spectroscopy (FT-IR)

The functional groups in the samples were determined by using a Nicolet 6700 infrared spectrometer. The sample was mixed with KBr with sample: KBr ratio of 1:100 and formed into a thin pellet, before measurement. The spectra were recorded at wavenumber between 400 and 4000 cm^{-1} with resolution of 4 cm^{-1} . The number of scan for the measurement was 64.

3.5.3 Thermogravimetric Analysis (TGA)

The residual carbon content and thermal behavior of the samples were determined by using thermogravimetric analysis on a SDT Q600 instrument. The analysis was performed from temperature of 50 to 1,000°C under a heating rate of 10°C/min in 100 ml/min flow of either oxygen or nitrogen.

3.5.4 Scanning Electron Microscopy (SEM)

Morphology of the products was examined by using a scanning electron microscope (JSM-6400, JEOL Co., Ltd.) at the Scientific and Technological Research Equipment Center (STREC), Chulalongkorn University.

3.5.5 Transmission Electron Microscope (TEM)

The morphology of an individual grain in the samples was observed on a JEOL JEM-2100 Analytical Transmission Electron Microscope, operated at 80-200 keV at the Scientific and Technological Research Equipment Center (STREC), Chulalongkorn University and JSM 2010 Analytical Transmission Electron Microscope at National Metal and Materials Technology Center, Thailand. The crystallographic information was also obtained from the selected area electron diffraction (SAED) analysis performed in the same instrument.

3.5.6 Surface Area Measurement

BET surface area of products was measured by Micromeritics ChemiSorb 2750 and Micromeritics ASAP 2020 at Center of Excellence on Catalysis and Catalytic Reaction Engineering laboratory, Chulalongkorn University. For this measurement nitrogen gas was used as the adsorbate.

3.5.7 Gas Chromatography

A gas chromatography, Shimadzu modal 8A (GC-8A) equipped with a thermal conductivity detector (TCD), was used to analyze gas composition during the carbothermal reduction and nitridation process. Nitrogen, hydrogen and carbon monoxide in the gas-outlet stream from the tubular flow reactor were analyzed using Molecular sieve 5A column, while carbon dioxide was analyzed by using Poropak-Q column. The operating conditions for the gas chromatography are shown in Table 3.1.

Table 3.1 Operating conditions for gas chromatograph

Gas Chromatograph	Shimadzu GC-8A	
Detector	TCD	
Column	Molecular sieve 5A	Porapak-Q
- Column material	SUS	SUS
- Length (m)	2	-
- Outer diameter (mm)	4	-
- Inner diameter (mm)	3	-
- Mesh range	60/80	-
- Maximum temperature (°C)	350	-
Carrier gas	Ar (99.999%)	Ar (99.999%)
Carrier gas flow (ml/min)	30	30
Column temperature		
- initial (°C)	70	70
- final (°C)	70	70
Injector temperature (°C)	100	100
Detector temperature (°C)	100	100
Current (mA)	70	70
Analyzed gas	N ₂ , H ₂ , CO	CO ₂

CHAPTER IV

RESULTS AND DISCUSSION

4.1 Preliminary Experiments

In preliminary experiments, silicon nitride synthesis according to the proposed approaches was validated by comparing products from the carbothermal reduction and nitridation of carbonized RF gel with and without silicon precursor. RF gel was prepared by sol-gel polycondensation according to procedures reported in literature (Tonanon et al. 2005) and APTMS was used as a precursor of silicon. Figure 4.1 shows XRD of the products after the nitridation. According to the XRD analysis, the RF carbon gel after nitridation is amorphous phase, while the nitrided product of the carbonized RF gel with APTMS is α -silicon nitride.

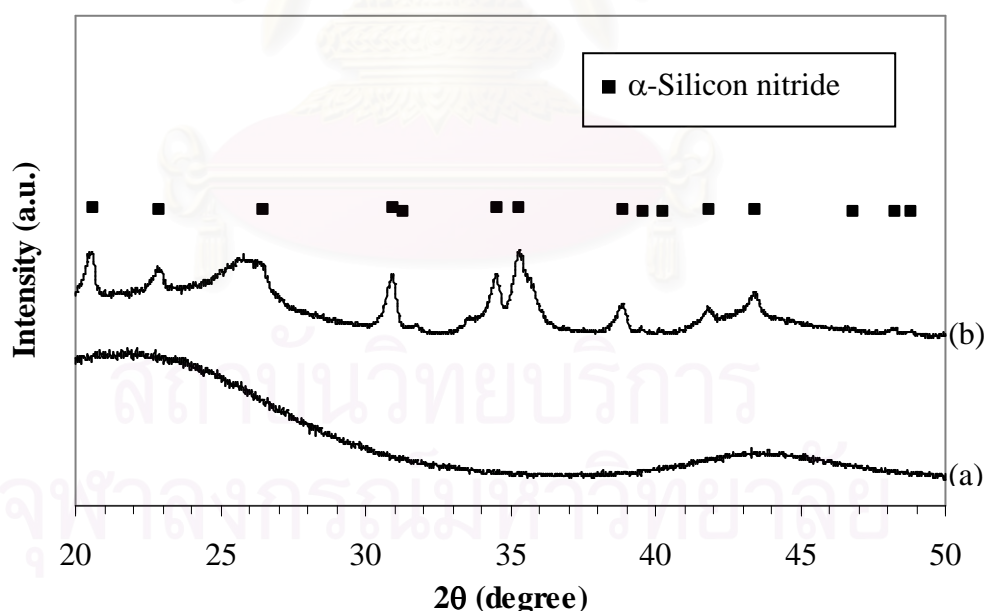
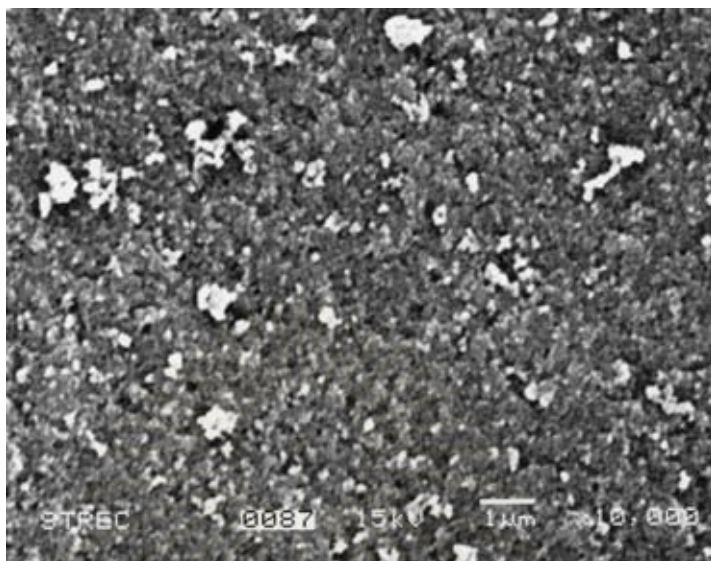
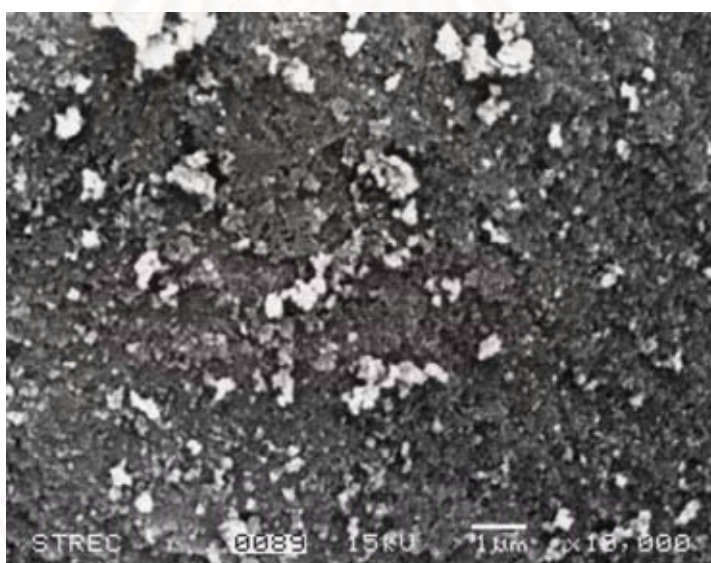


Figure 4.1 XRD patterns of nitrided powders obtained by using:
(a) pure RF carbon gel (b) RF carbon gel with APTMS.



(a)



(b)

Figure 4.2 SEM micrographs of RF carbon gel (a) before nitridation and (b) after nitridation.

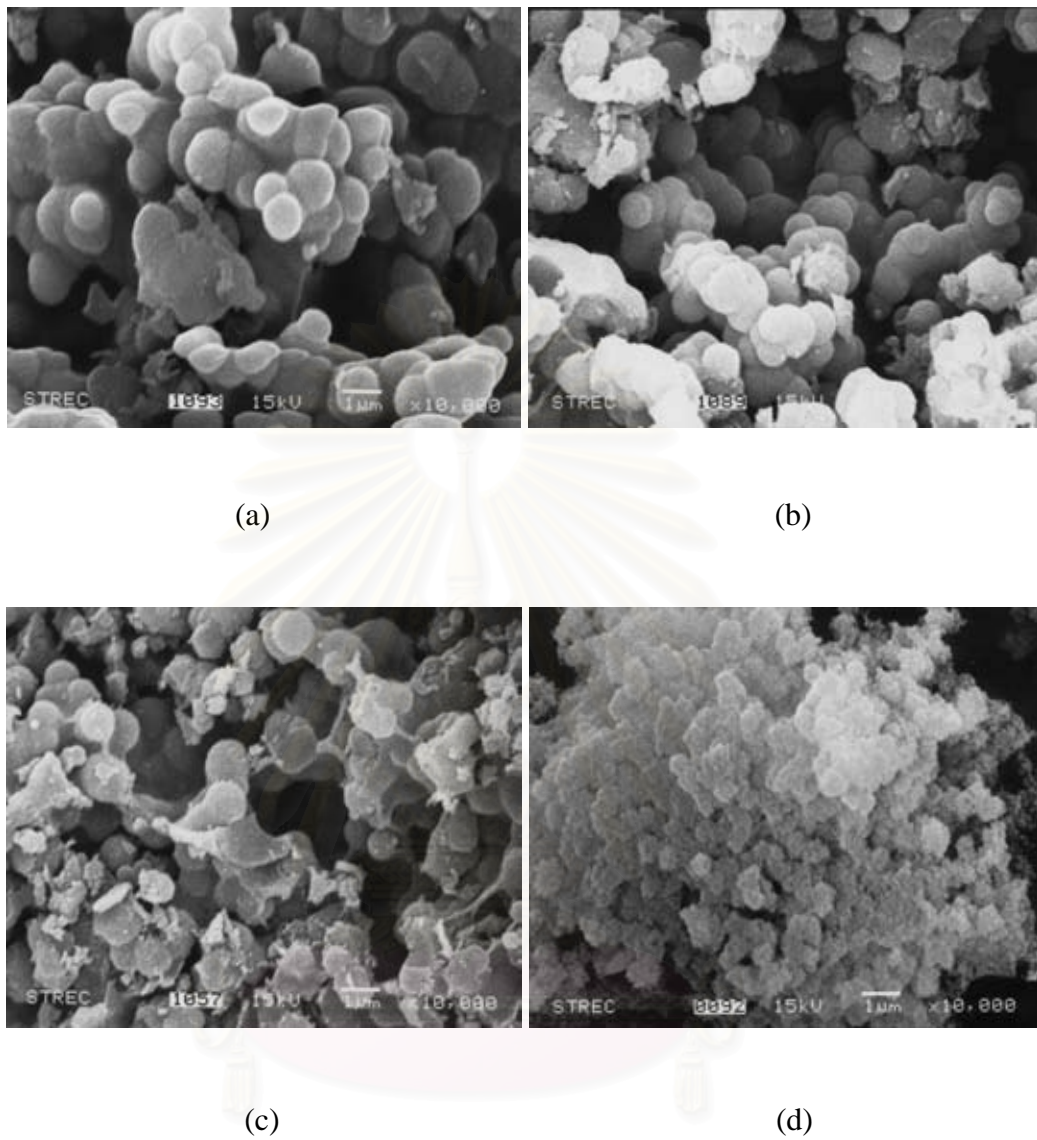


Figure 4.3 SEM micrographs of silica/RF composite with the Si/C ratio of 0.07:

- (a) before pyrolysis, (b) after pyrolysis, (c) after nitridation and
(d) after calcination

Figure 4.2 shows SEM micrographs of RF carbon gel before and after nitridation. It can be seen that the nitrided product has same porosity and morphology as the original RF carbon gel. Similar observation was also found in the case of powder prepared with silicon source (APTMS). As shown by SEM micrographs in Figure 4.3 (a) to (c), silica/RF gel before pyrolysis, silica/carbon composite obtained after pyrolysis and the nitrided product have same morphology, all of which are consisting of grains with uniform size. This result indicates that the structure, morphology as well as porosity of subsequent products depend upon the formation of silica/RF gel. BET surface area of the product obtained after pyrolysis ($334.29 \text{ m}^2/\text{g}$) and that obtained after nitridation ($331.31 \text{ m}^2/\text{g}$) are not different because both products still contain high carbon content. On the other hand, the final product after calcination (Figure 4.3 (d)) has lower surface area ($99.14 \text{ m}^2/\text{g}$) because carbon content was burned out and only silicon nitride remains in the sample. Therefore, it can be concluded that the residual carbon in the sample contributes to large fraction of the measured surface area.

Figure 4.4 shows the results for TGA analysis of silica/RF gel in nitrogen atmosphere. This analysis simulates the pyrolysis process that converts silica/RF gel to silica carbon composite. The results indicate that about 45 wt% of organic compound is lost during pyrolysis. Further TGA analysis of silica carbon composite was done in oxygen atmosphere. The results (Figure 4.5) suggest that there is approximately 20 wt% of silica in the composite. The rest is residual carbon in the sample.

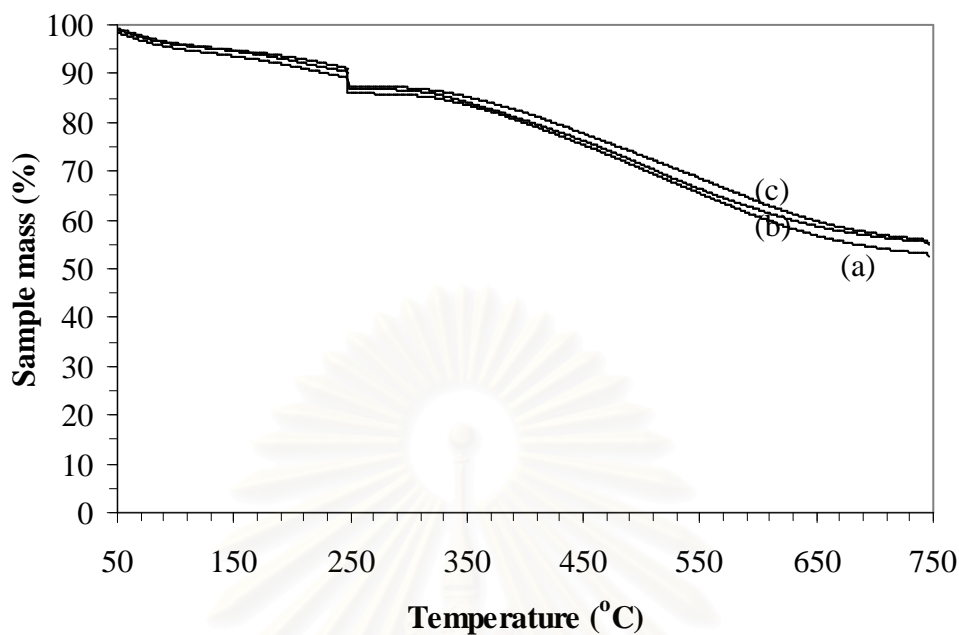


Figure 4.4 TGA analysis in nitrogen atmosphere of silica/RF gel at various molar ratios of silicon and carbon: (a) Si/C = 0.03, (b) Si/C = 0.05 and (c) Si/C = 0.07.

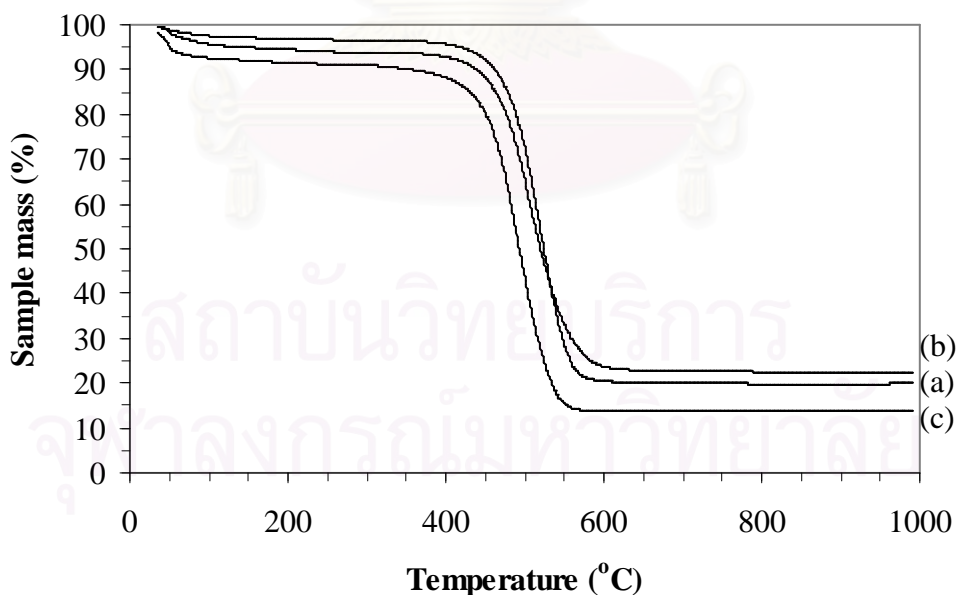


Figure 4.5 TGA analysis in oxygen atmosphere of pyrolyzed silica/RF gel at various molar ratios of silicon and carbon: (a) Si/C = 0.03, (b) Si/C = 0.05 and (c) Si/C = 0.07.

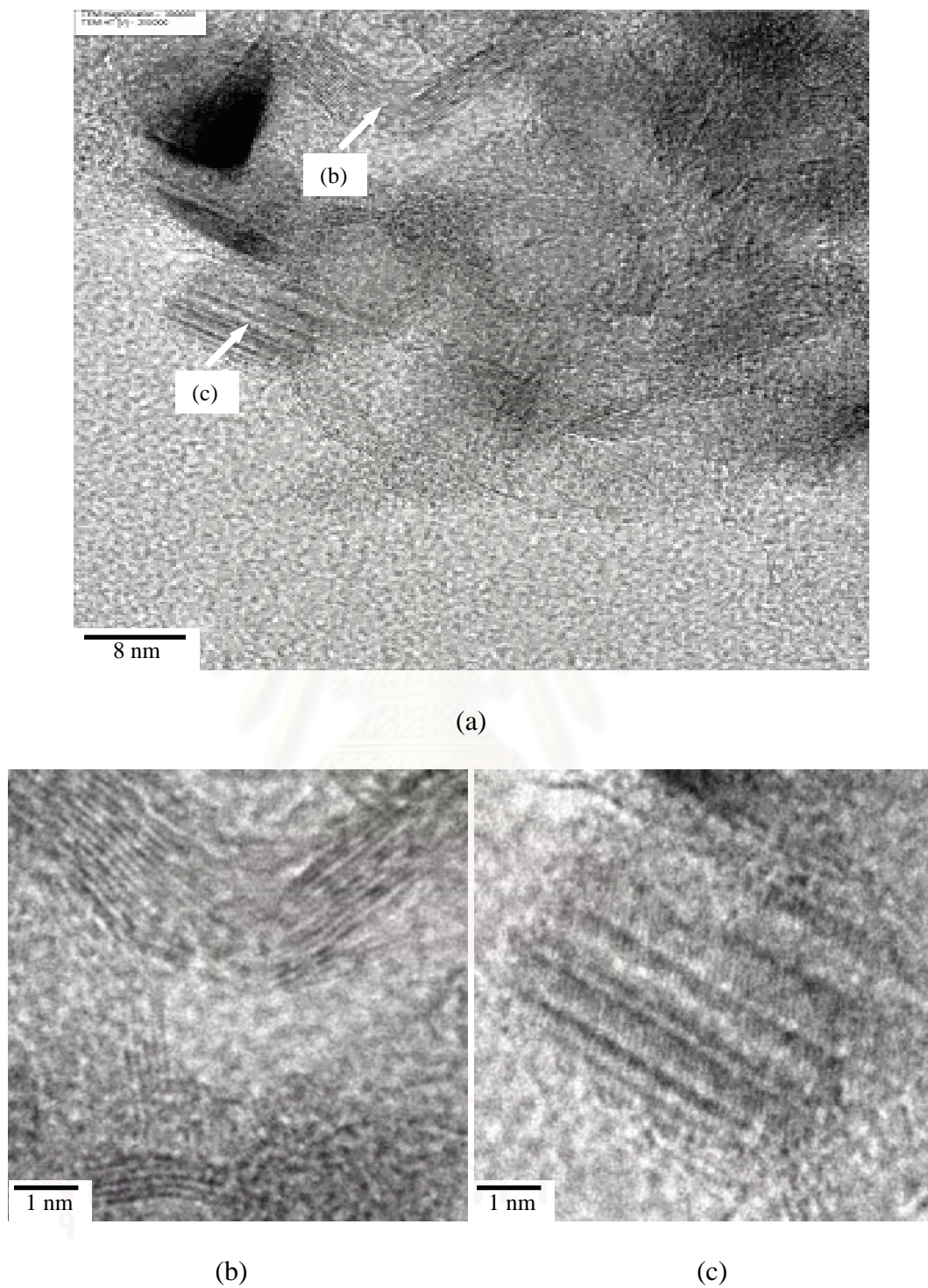


Figure 4.6 TEM micrographs of the nitrided product with molar ratio of Si/C = 0.05: (a) nitrided powder, (b) graphite and (c) silicon nitride.

Figure 4.6 shows TEM micrograph of the nitrated powder with molar ratio of Si/C = 0.05, prepared without solvent exchange. It should be noted that sample shown in this Figure has not been calcined. In this Figure, lattice fringes are clearly seen. Nevertheless, close examination reveals two types of crystalline material. The first one shows curved features with lattice spacing of 0.375 nm (Figure 4.6(b)), which is expected to be carbon in graphite form (Trassl et al. 2002). The other material is silicon nitride with the lattice spacing of 0.193 nm (Figure 4.6(c)).

The results from preliminary experiments confirm that silicon nitride can be synthesized from silica/RF composite when APTMS is used as silica precursor. The morphology of the resulting powder depends on the formation and composition of silica/RF gel. Further experiments were conducted to find suitable precursor of silica for the synthesis of porous silicon nitride, as well as effects of several factors on properties of the obtained products.

4.2 Effect of Silica Precursor

In this work, three silica precursors, i.e. APTMS, TEOS and sodium silicate were investigated. Silica/RF gel composite powder was prepared by sol-gel and co-polymerization process with an addition of silica precursor. The results from the X-ray diffraction analysis of the final nitrated products after calcination are shown in Figure 4.7.

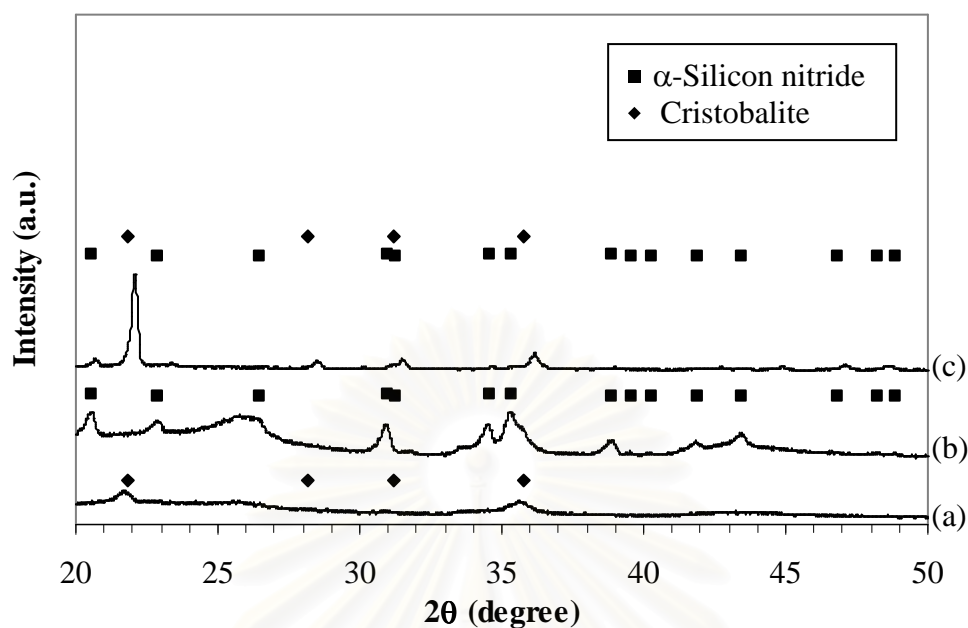


Figure 4.7 XRD patterns of nitrated powders obtained after calcination at 700°C for 10 h when various kinds of silica precursor are used: (a) TEOS (b) APTMS and (c) Sodium silicate.

From the XRD analysis, it can be observed that α -silicon nitride can be synthesized only when APTMS is used as silica precursor. The nitrated products of silica/RF gel using TEOS and sodium silicate as the precursor are silica in cristobalite phase. Figure 4.8 shows FT-IR spectra of silica/RF composite with various silica precursors. Anti-symmetric and symmetric stretching vibrations of Si-O-Si bonding (referring to silica) are observed at wave number of 1,100 and 800 cm^{-1} in all samples. In addition, the sample that used TEOS or sodium silicate as precursor shows amorphous silica band at 570 cm^{-1} (Karmakar et al. 2000). However, it is anticipated that APTMS has a suitable structure to form crosslinked Si-O-Si network during the sol-gel process, while TEOS and sodium silicate may not be appropriate silicon source because they result in amorphous silica form that transforms to cristobalite at temperature in the range of 1,000-1,200°C (Kamiya et al. 1990). It has been generally accepted that cristobalite is the most chemically stable form of silica. Thus, once cristobalite is formed, silica in the composite can not be reduced to intermediate SiO, which is essential for the formation of silicon nitride during the carbothermal reduction and nitridation (Matovic 2003).

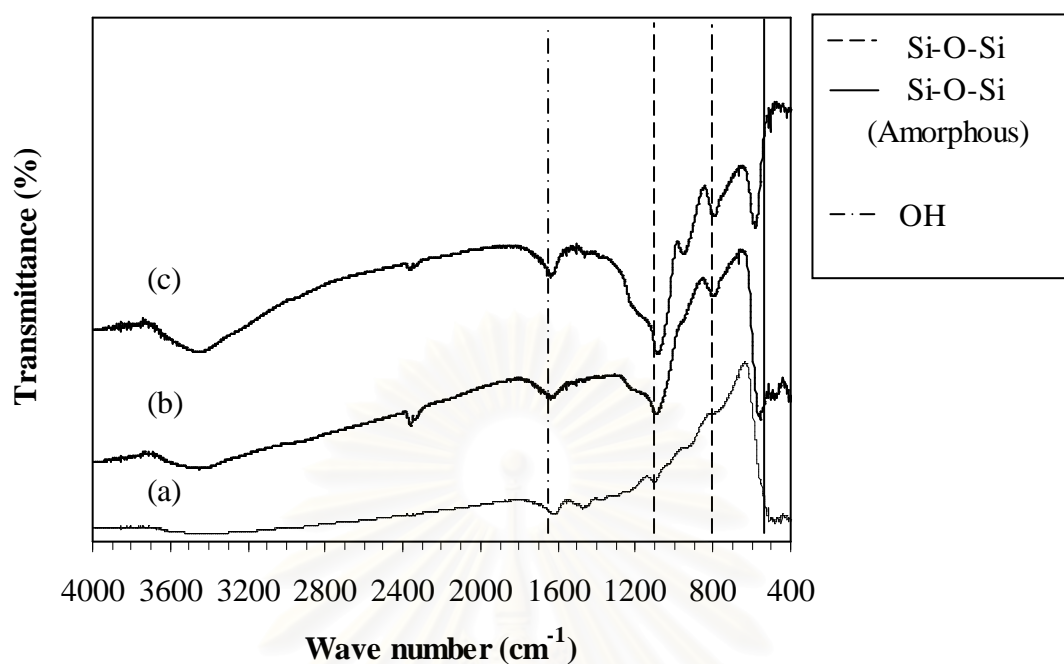


Figure 4.8 FT-IR spectra of silica/RF composite that uses (a) APTMS, (b) sodium silicate and (c) TEOS as precursor of silica.

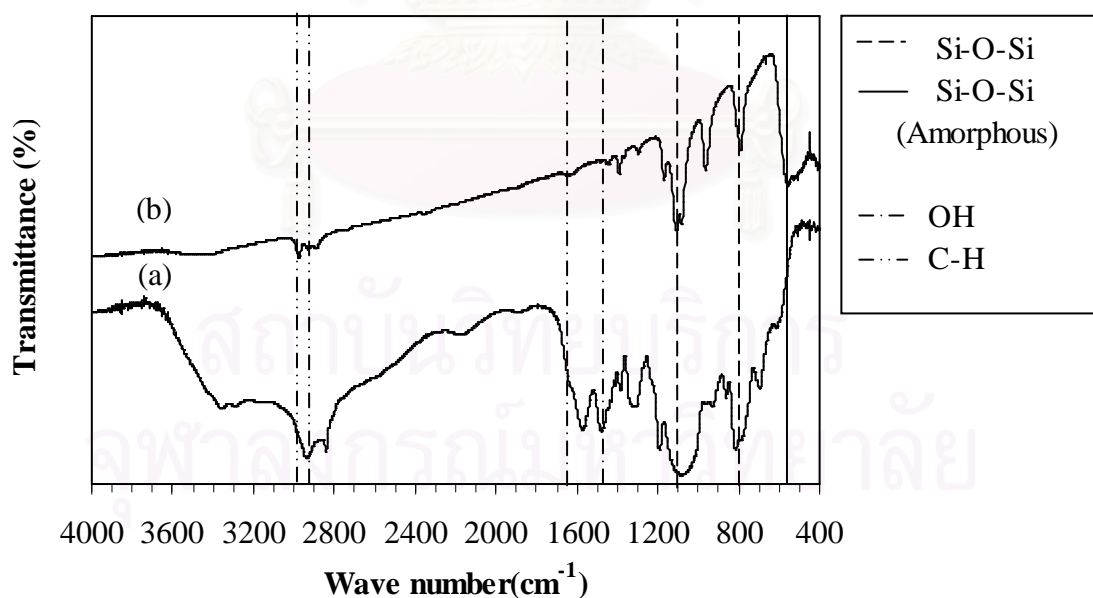


Figure 4.9 FT-IR spectra of silica precursor used in the preparation of silica/RF composite: (a) APTMS and (b) TEOS.

FT-IR spectra of APTMS and TEOS which were used as silica precursor in the preparation of silica/RF composite are shown in Figure 4.9. These spectra have the same silica absorption bands as observed in Figure 4.8. The differences come from C-H and the other organic band. The FT-IR analysis results indicate that, during the formation of silica/RF composite, the organic bands of APTMS and TEOS disappear.

4.3 Effect of Si-to-C Ratio on Properties of Silicon Nitride

Figure 4.10 shows FT-IR spectra of silica/carbon composite after pyrolysis (before nitridation) at various Si/C molar ratios. It is shown that all silica/carbon composites have absorption bands at wave number of 800 and 1100 cm^{-1} , which are corresponding to Si-O-Si bonding. These results confirm the presence of silica in all pyrolyzed samples. It should also be noted that the signals for Si-O-Si bonding are more pronounced in the sample with high Si/C ratio.

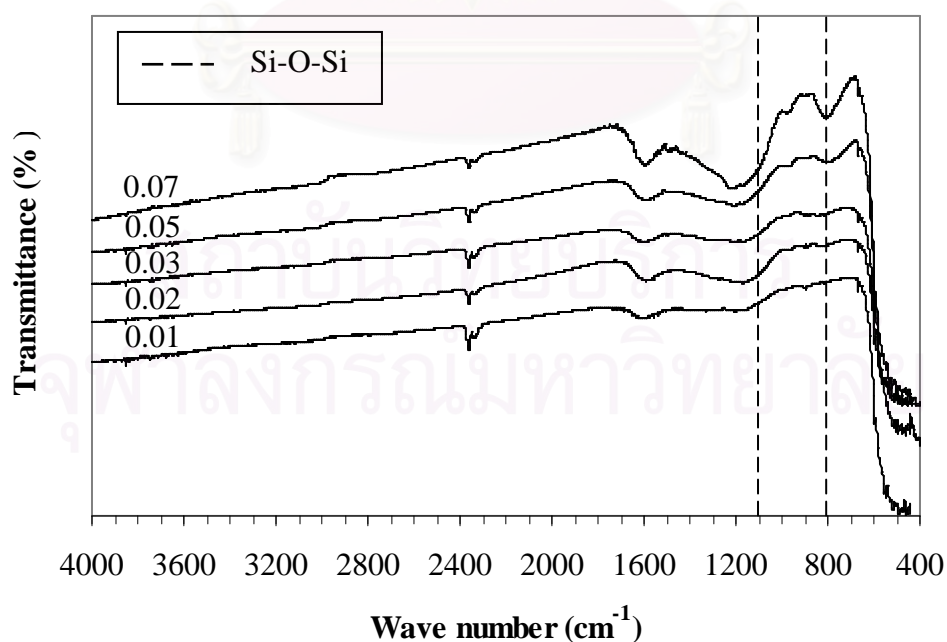


Figure 4.10 FT-IR spectra of silica/carbon composite at various molar ratios of Si/C.

Figure 4.11 is XRD analysis results for silicon nitride powder obtained from silica/RF composite with various molar ratios of silicon to carbon. The results confirm that the product obtained after calcination was silicon nitride, mainly in α -phase. No other crystalline phase was detected. Table 4.1 shows BET surface area of silicon nitride powder synthesized in this section. It is seen that all products synthesized in this work have much higher surface area than the conventional silicon nitride granules, which indicates significant increase in porosity. The surface area is increased when amount of silica precursor is increased. At the Si-to-C ratio of 0.01, the powder has the lowest surface area because it contains silica in low content, but has high amount of carbon. Small amount of silica results in weak pore structure of the obtained silicon nitride. Subsequently, the pore collapse during calcination process where carbon in the sample is removed, causing the decrease in surface area of the sample. Higher the Si/C ratio leads to the stronger pore structure, which prevents pore collapsing and retains high surface area after calcination. The surface area of the obtained product reached maximum at Si/C molar ratio of 0.05. At the molar ratio higher than 0.05, silica in the silica/carbon composite agglomerates and yields large silicon nitride grains, which decreases the surface area. This can be confirmed by shows SEM micrographs of the silicon nitride powders after calcination that were synthesized from silica/RF composite with various molar ratios of Si/C (Figure 4.12). The results also indicate that silicon nitride synthesized in this work is consisted of uniform grains, which are smaller than that in the conventional silicon nitride.

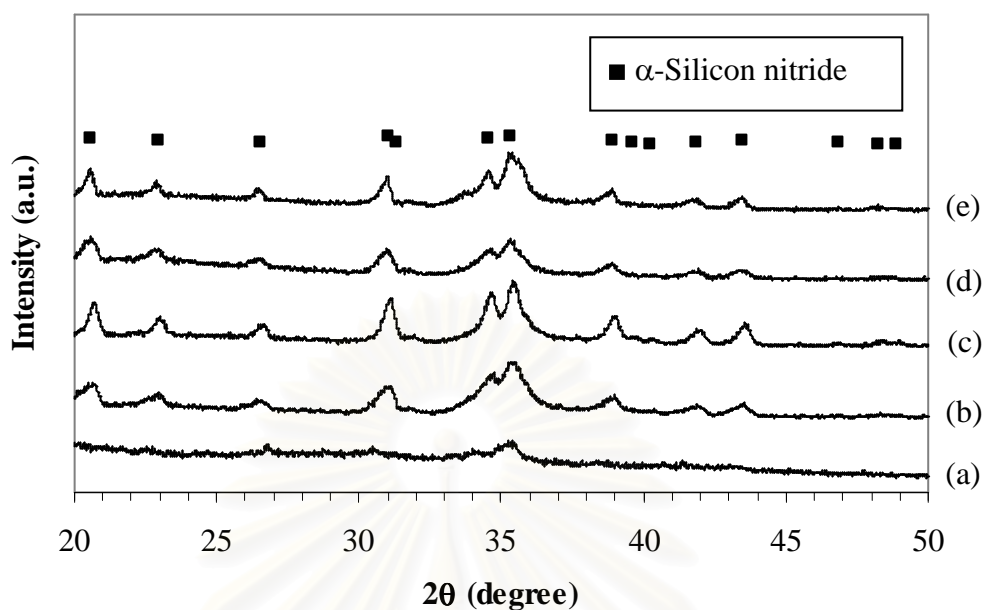


Figure 4.11 XRD patterns of silicon nitride powder synthesized with various Si/C molar ratios, after calcination at 700°C for 10 h:(a) 0.01; (b) 0.02; (c) 0.03; (d) 0.05 and (e) 0.07.

Table 4.1 Surface area of silicon nitride powder synthesized with various Si/C molar ratios after calcination.

Si/C molar ratio	Surface area (m ² /g)	
	with solvent exchange	without solvent exchange
0.01	69.57	60.95
0.02	74.64	62.00
0.03	183.01	163.51
0.05	212.63	204.29
0.07	99.14	78.73
Commercial silicon nitride*	1.2-13.0	

* Source: PRED Materials international, Inc.

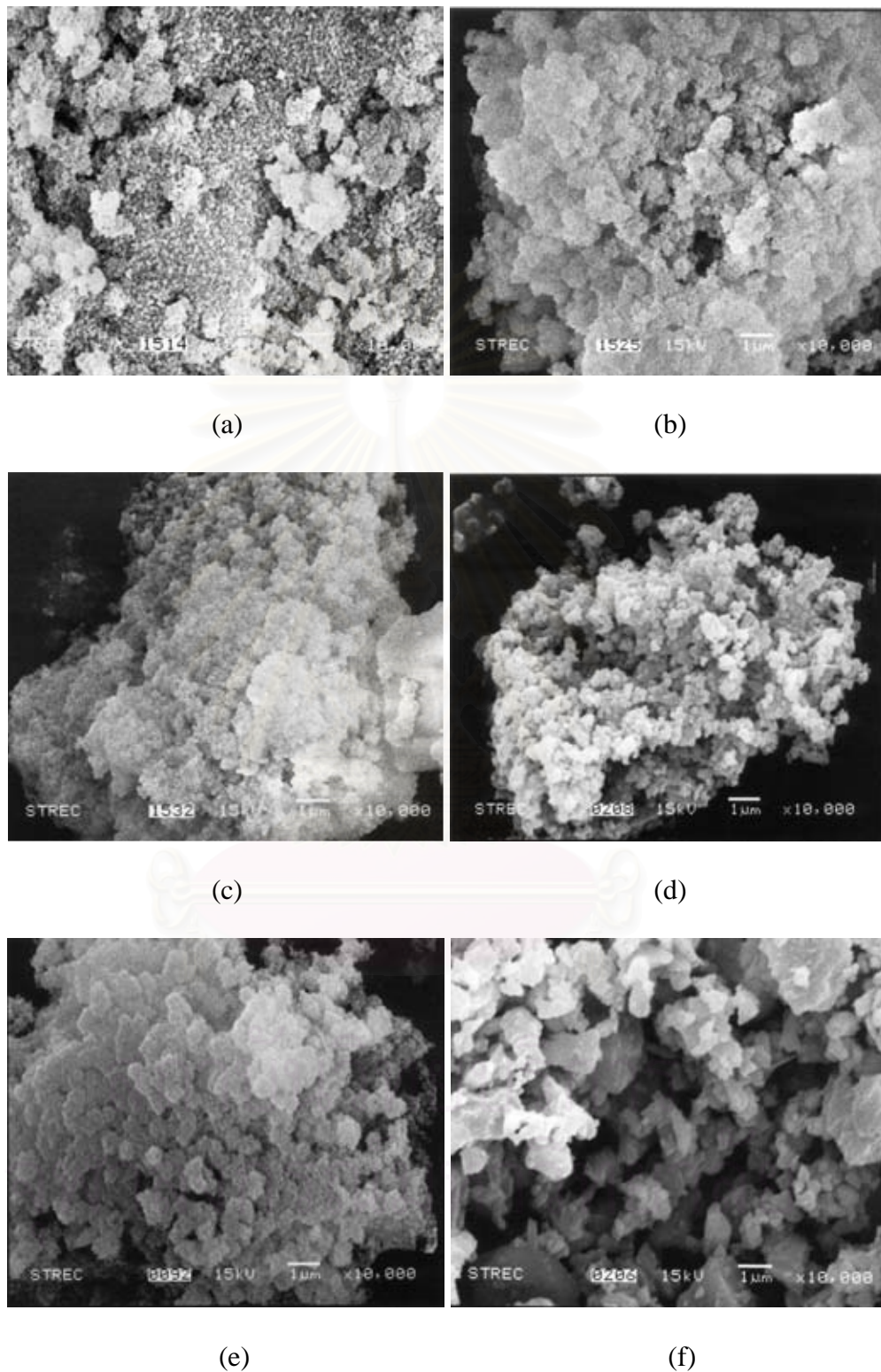


Figure 4.12 SEM micrographs of the silicon nitride synthesized with various Si/C molar ratios, after calcination: (a) 0.01; (b) 0.02; (c) 0.03; (d) 0.05; (e) 0.07 and (f) conventional silicon nitride powder.

Results from TGA analysis in oxygen shown in Figure 4.13 suggest that majority of residual carbon can be removed by calcination. All calcined samples reveal no significant mass decrease during the TGA analysis. Only small amount of carbon remaining in the product after calcination is observed in samples with high carbon content, i.e. samples synthesized with Si/C of 0.03 and 0.05. On the other hand, for the sample with low carbon (i.e. high silicon content), slight mass increase is observed at the analysis temperature higher than 700°C. This is the result from surface oxidation of silicon nitride.

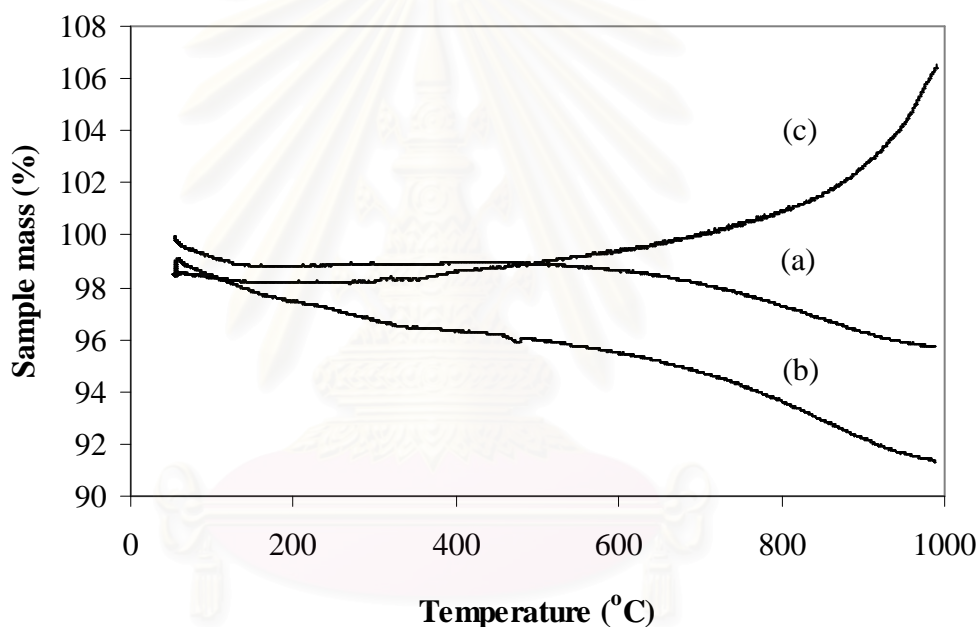


Figure 4.13 TGA analysis of the final products after calcination process with various molar ratios of silicon- to-carbon: (a) Si/C = 0.03, (b) Si/C = 0.05 and (c) Si/C = 0.07.

4.4 Effect of Solvent Exchange on Properties of Silicon Nitride

The results in Table 4.1 also show effect of the method to remove water from the silica/RF composite on the surface area of the silicon nitride porproduct. The product that was treated with *t*-butanol in the solvent exchange process has higher surface area than the product that was dried without solvent exchange. Since water has high surface tension, removal of water from a pore by direct drying can cause the pore structure to collapse by capillary force. On the other hand, water removal by exchanging with *t*-butanol, before subsequently drying, can prevent such effect because *t*-butanol has lower surface tension. Figure 4.14 and 4.15 show SEM micrographs of silica/RF composite after drying (before pyrolysis) and the silicon nitride powder after calcination process respectively. Figure 4.14(a) and 4.15(a) show microstructures of powder which was prepared with solvent exchange. Figure 4.14(b) and 4.15(b) show microstructures of powder prepared without solvent exchange. It is clearly seen that the powder prepared without solvent exchange is more compact than the powder prepared with solvent exchange. It is also shown that solvent exchange process results in uniform grains of the particles. The powders formed without solvent exchange are agglomerated.

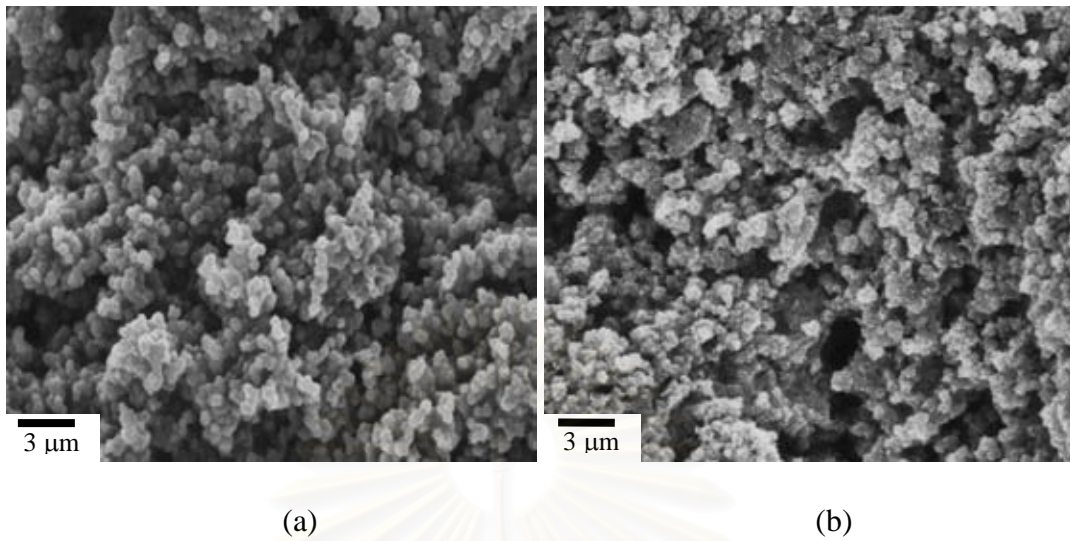


Figure 4.14 SEM micrographs of silica/RF composite with Si/C ratio of 0.07, before pyrolysis: (a) prepared with solvent exchange; (b) prepared without solvent exchange.

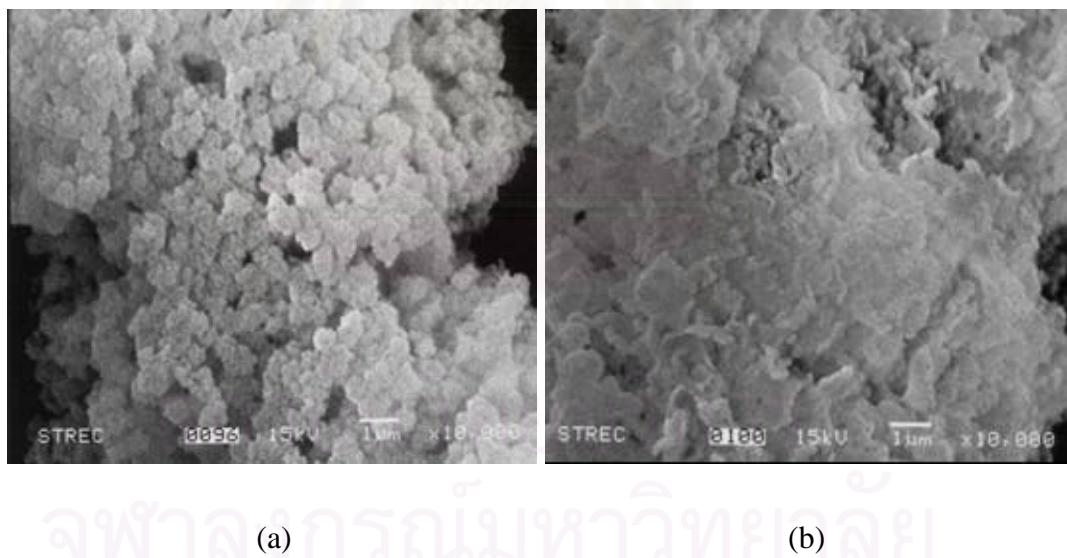


Figure 4.15 SEM micrographs of the silicon nitride powder with Si/C ratio of 0.07, after calcined: (a) prepared with solvent exchange, (b) prepared without solvent exchange.

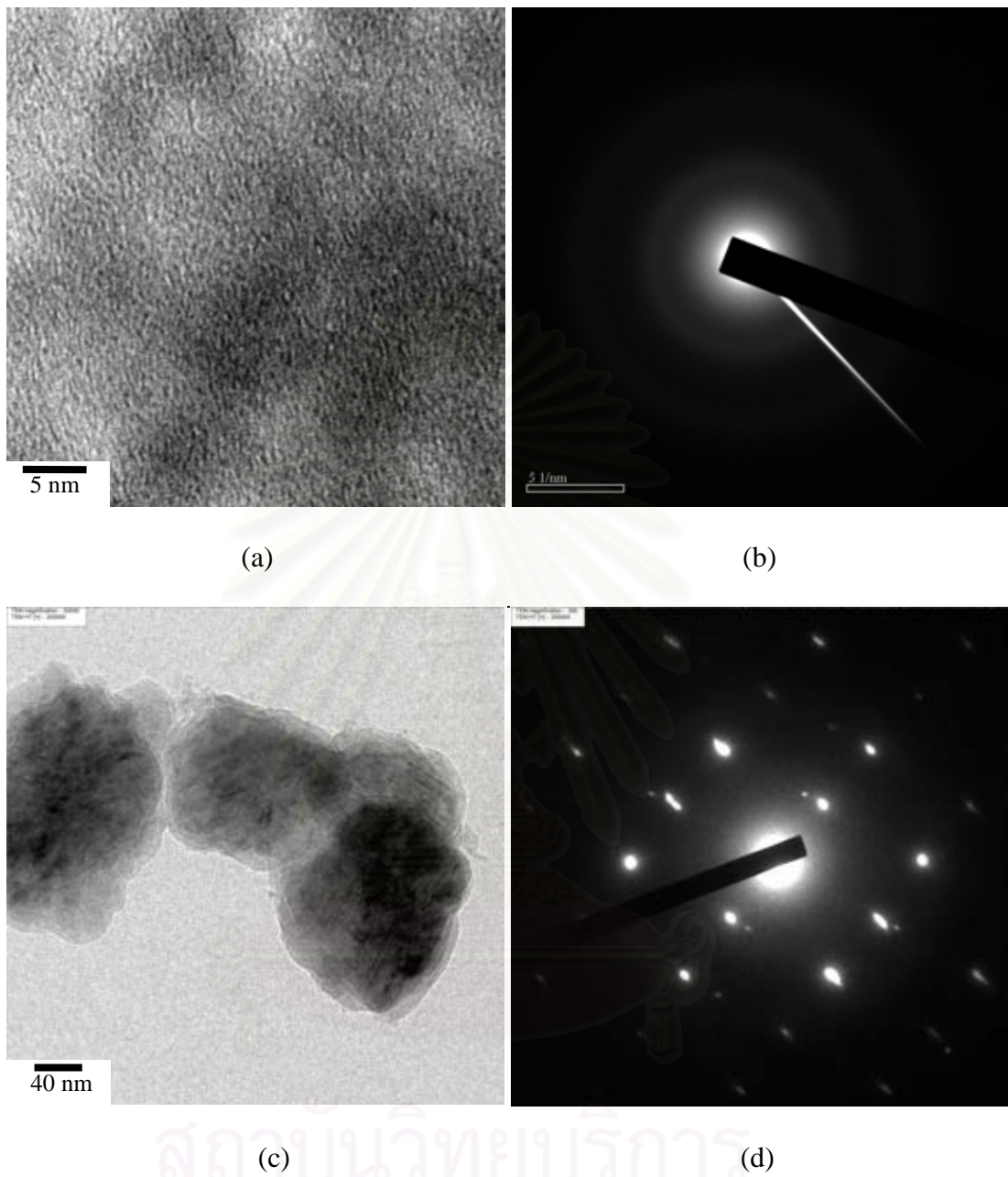
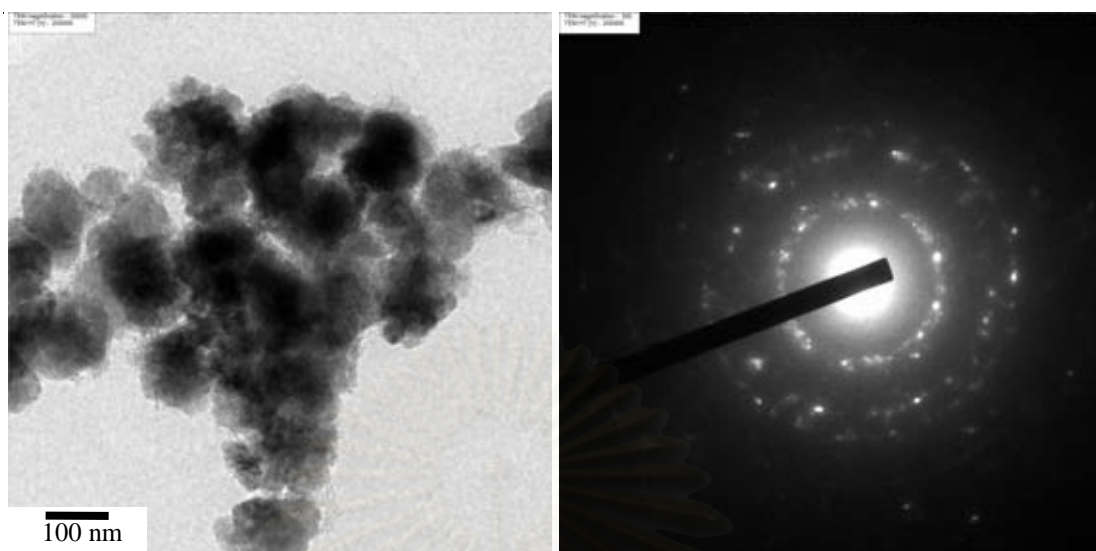
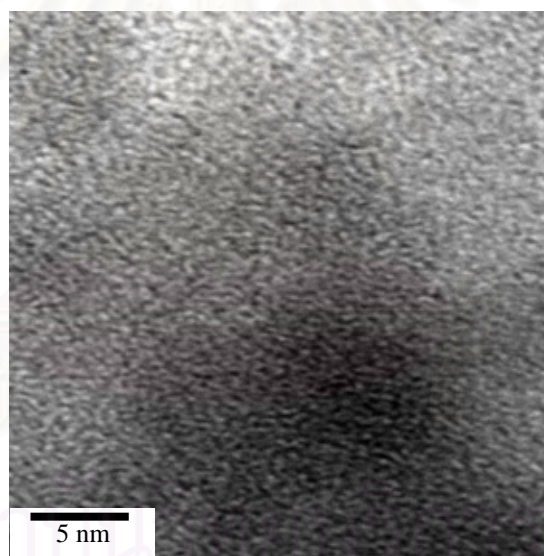


Figure 4.16 TEM micrographs and SAED patterns of the silicon nitride powder synthesized with Si/C molar ratio = 0.05 without solvent exchange, after calcination process: (a) amorphous phase, (b) SAED of amorphous phase, (c) crystal silicon nitride and (d) SAED of crystal silicon nitride.



(a)

(b)



(c)

Figure 4.17 TEM micrographs and SAED pattern of the silicon nitride powder synthesized with Si/C molar ratio = 0.05 with solvent exchange, after calcination process.

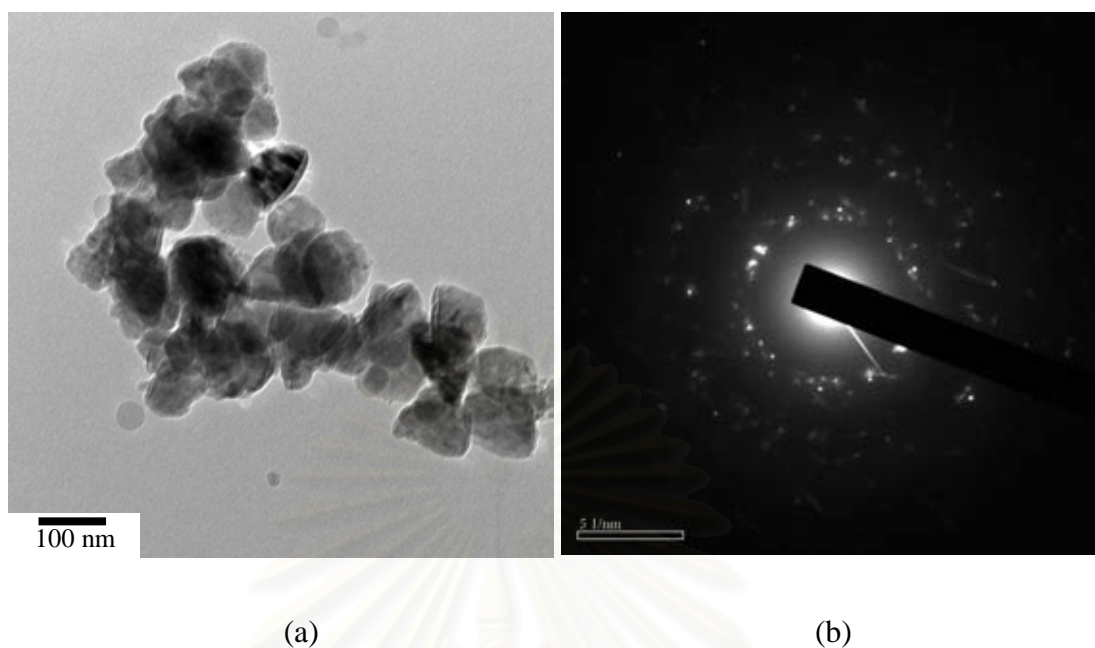


Figure 4.18 TEM micrograph and SAED pattern of the silicon nitride powder synthesized with Si/C molar ratio = 0.07 without solvent exchange, after calcination process.

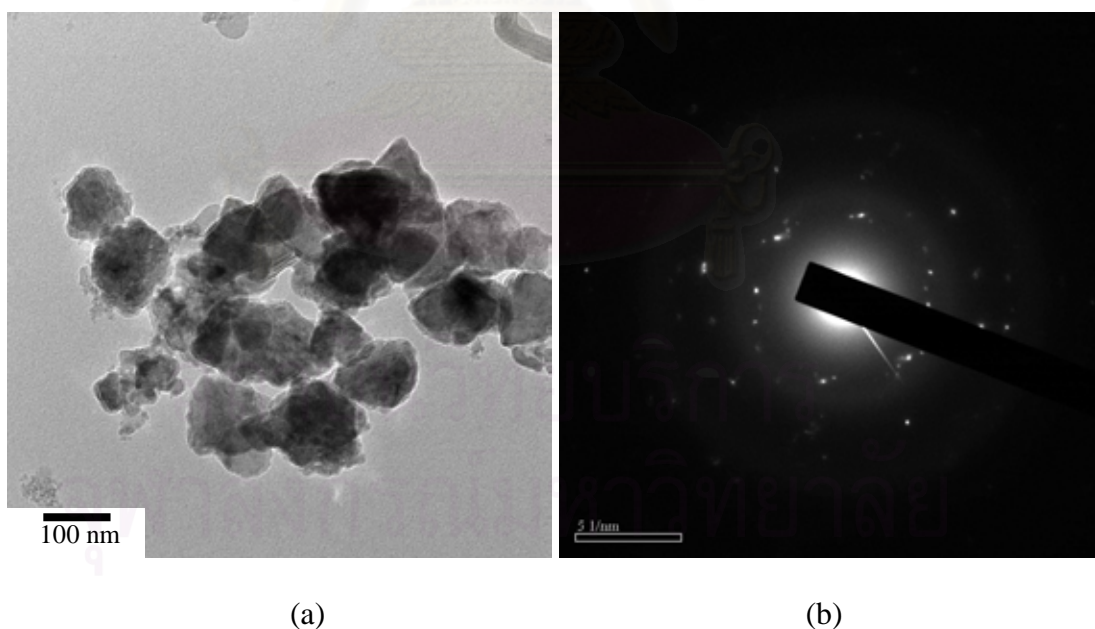


Figure 4.19 TEM micrograph and SAED pattern of the silicon nitride powder synthesized with Si/C molar ratio = 0.07 with solvent exchange, after calcination process.

Figure 4.16-4.19 show TEM micrographs and SAED patterns of silicon nitride after calcination process. According to Figure 4.16, in which silicon nitride was synthesized with Si/C ratio of 0.05, the product consists of both amorphous and crystal phase. SAED pattern of Figure 4.16(a) shown in 4.16(b) confirms the presence of amorphous in the sample. On the other hand, at different spot in the same sample, the product forms into single crystalline silicon nitride (Figure 4.16(c)-(d)). Similar observation was found on the sample processed with a step of solvent exchange, as shown in Figure 4.17. However, the crystal phase in this case is polycrystalline. At Si/C ratio of 0.07, majority of the sample is crystalline with high crystallinity, as evidenced for SAED patterns shown in both Figure 4.17 and 4.18.

It is suggested that amorphous phase observed from TEM in Figure 4.16(a) and 4.17(c) when silicon nitride was prepared with Si/C molar ratio of 0.05 may be free carbon (Trassl et al. 2002) residing in the obtained powder. This result is consistency with TGA analysis (Figure 4.13) because mass loss in silicon nitride comes from free carbon that was burned out of the sample.

For the products prepared with solvent exchange (Figure 4.17 and 4.19), the particle sizes of these products are not different, even though the Si/C ratio of the samples are different. On the contrary, for the samples prepared without solvent exchange, it can be clearly seen that particle size of silicon nitride in Figure 4.16(Si/C = 0.05) is bigger than Figure 4.18(Si/C = 0.07) However, surface area of silicon nitride powder obtained with Si/C molar ratio of 0.05 is higher than that of silicon nitride obtained from Si/C molar ratio of 0.07. The higher surface area is the result from amorphous phase presented in silicon nitride powder obtained with Si/C molar ratio of 0.05. It should also be noted that particles of products prepared without solvent exchange (Figure 4.16(c)) are more agglomerated than the product prepared with solvent exchange (Figure 4.17(a)).

4.5 Effect of Aging Time on Properties of Silicon Nitride

Figure 4.20 and 4.21 show pore size distribution of the calcined porous silicon nitride with the Si/C ratio of 0.05 and 0.07, respectively. All samples were prepared with the aid of solvent exchange. It can be seen that all samples share common feature in the pore size distribution, i.e. bimodal distribution with peaks around 40 and 200 angstroms, respectively. Regardless of the pore size distribution, it is conclusive that silicon nitride synthesized in this work is mesoporous.

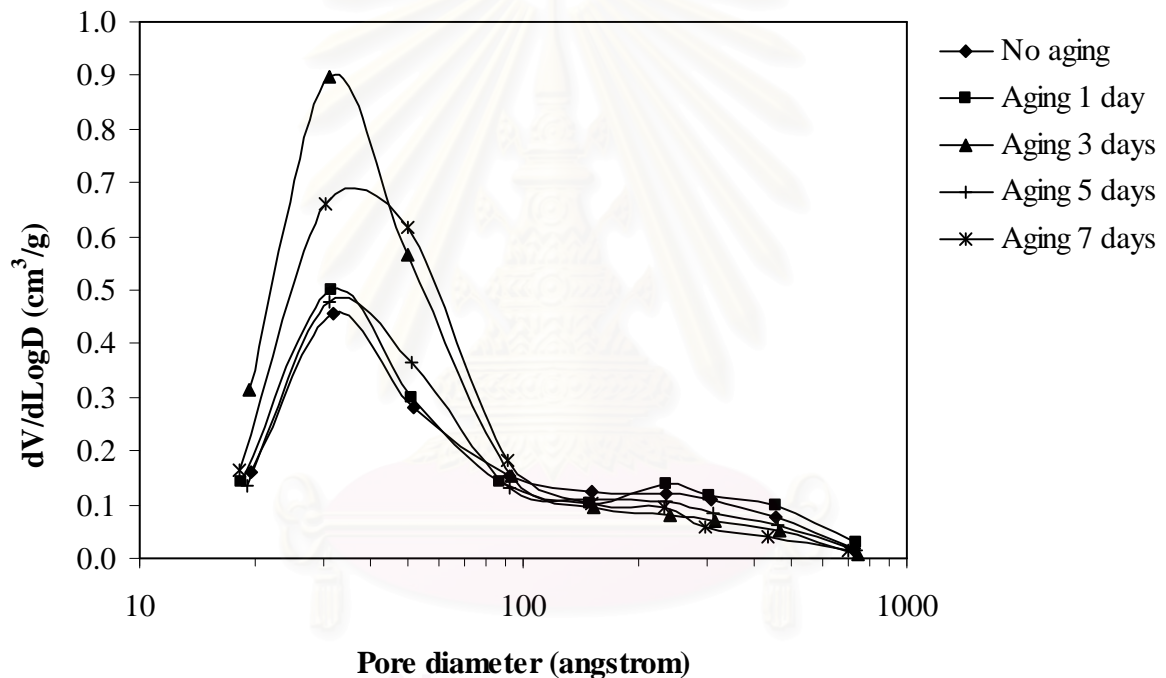


Figure 4.20 Pore size distribution of calcined silicon nitride powder prepared from silica/RF composite with Si/C ratio of 0.05, using various aging times.

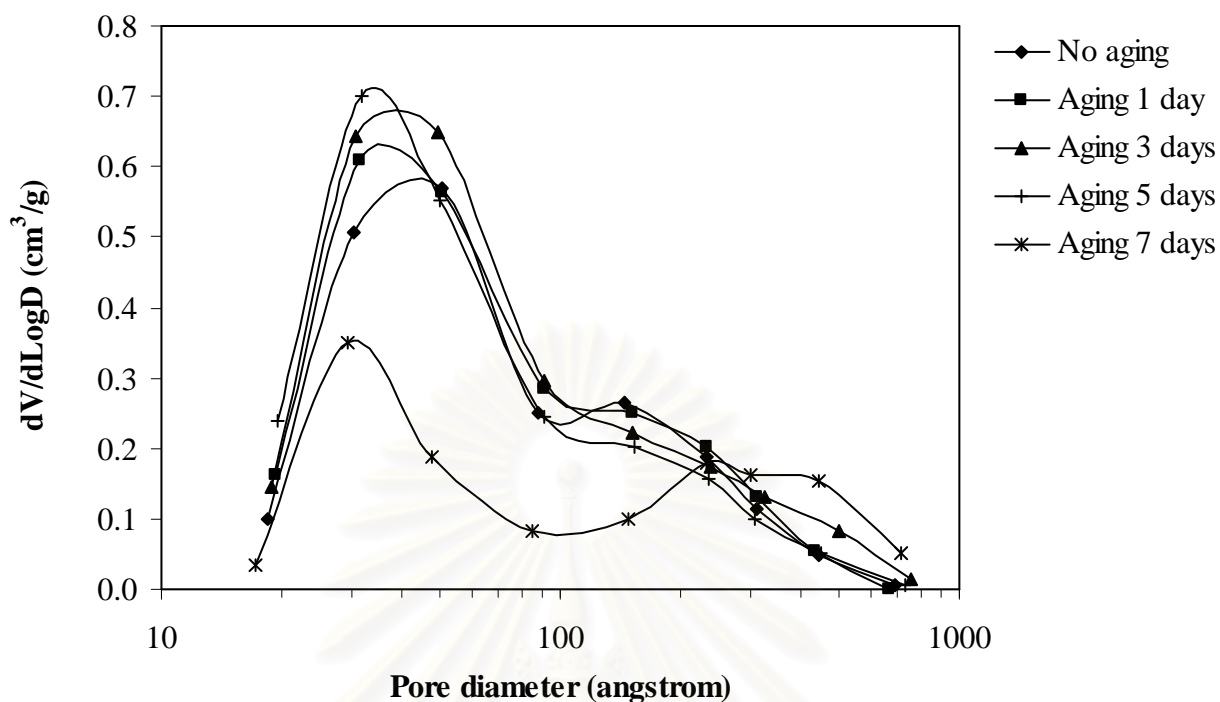


Figure 4.21 Pore size distribution of calcined silicon nitride powder prepared from silica/RF composite with Si/C ratio of 0.07, using various aging times.

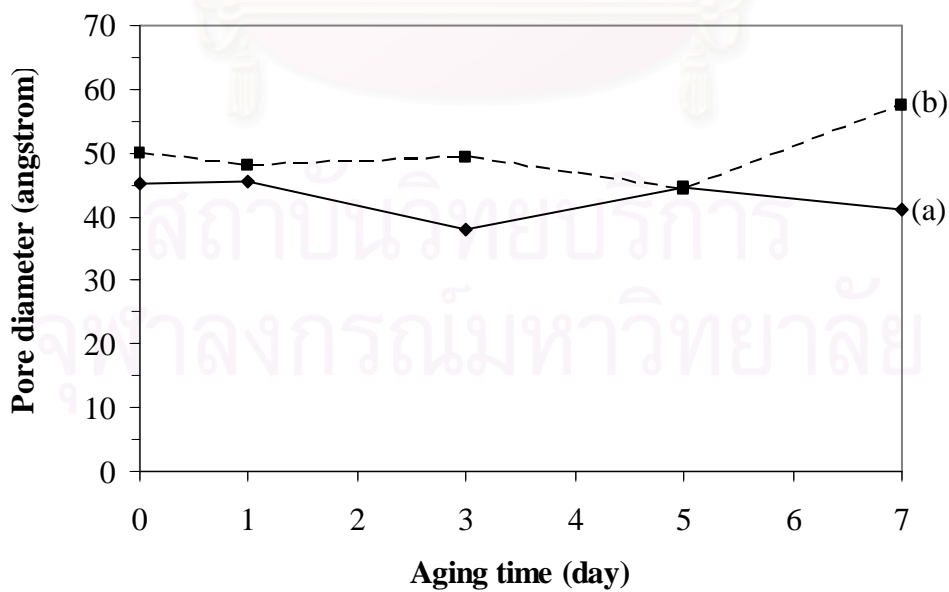


Figure 4.22 The average pore diameters of silicon nitride synthesized with various aging times: (a) Si/C molar ratio = 0.05 and (b) Si/C molar ratio = 0.07.

Table 4.2 Surface area of silicon nitride powder synthesized after calcination with various aging times.

Molar ratio Si/C	Aging time (day)	Surface area (m ² /g)
0.05	0	201.12
	1	211.86
	3	355.37
	5	200.77
	7	271.56
0.07	0	229.36
	1	281.80
	3	290.67
	5	316.43
	7	159.44

According to the results for samples with Si/C ratio of 0.05 (Figure 4.20) samples aged for, all of aging times investigated show one major peak around 30-40 angstroms and minor peak at pore size bigger than 100 angstroms. Table 4.2 shows BET surface area of calcined sample with Si/C molar ratio of 0.05 at various aging time. From these results, it is found that three days of aging results in porous silicon nitride with the highest surface area.

When silicon content is increased to Si/C ratio of 0.07, pores with size around 25-40 angstroms apparently get smaller as the aging time is increased, while large pores (e.g. larger than 100 angstroms) seems to grow larger. The growing in pore size of the large pores occurs because gel forms into bigger particle, when it is aged for long time. The highest surface area at this molar ratio is obtained after five days of aging.

Figure 4.22 shows average pore diameters of silicon nitride synthesized with various aging times. In general, aging time of the silica/RF gel composite dose not influence the average pore diameter of the silicon nitride powder. Nevertheless, the

aging time has effect on strength of the silica/RF gel network. It can be seen that from Figure 4.21 small pores in sample, which was aged for long time, remain very small even after the nitridation at high temperature. It is suggested that strong structure of silica/RF gel is developed during aging time. It can tolerate severe synthesis processes without shrinkage or cracking (Husing and Schubert 2005) and remains as mesoporous structure in the final products.

4.6 Effect of pH on Properties of Silicon Nitride

The gelling time of RF solution is affected by pH of the solution (Aguado-Serrano et al. 2004). The same effect is also found in the preparation of silica /RF composite. The lower pH of RF solution gives the longer gelling time. This behavior is similar to that reported by Aguda-Serrano et al. (2004). For silicon nitride prepared from silica/RF composite with Si/C molar ratio of 0.05 at pH 3.0, 4.0 and 5.0, the pore size distribution are shown in Figure 4.23. It is obvious that pH value has effect on pore size of the silicon nitride powder. The powder synthesized at pH 3.0 has wide pore size distribution, in the range of 14-600 angstroms. Lin and Ritter (1997) also found that a lower pH tended to produce a broader pore size distribution in xerogels. At pH 4.0 the pore size distribution shows two peaks around 41 and 235 angstroms. However, when pH of the silica/RF composite is kept at 5.0, the obtained silicon nitride powder shows wide pore size distribution. Figure 4.23(d) also shows pore size distribution of carbon derived from RF gel without addition of APTMS. The result indicates that it is mesoporous with the diameter of pore larger than that of silicon nitride powder.

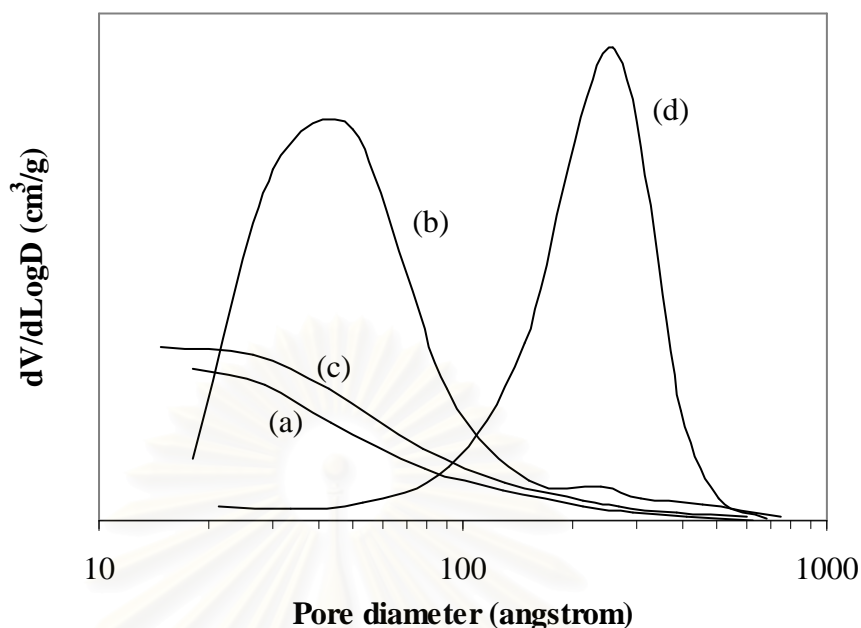


Figure 4.23 Pore size distribution of the calcined silicon nitride powders, which were synthesized from silica/RF composite prepared at different pH value: (a) pH = 3.0, (b) pH = 4.0 and (c) pH = 5.0; and RF carbon (d) prepared at pH = 7.4

The pH of RF solution and APTMS are 7.0 and 8.0, respectively. The silica/RF solution obtained after mixing RF solution and APTMS together has pH around 7.0. When pH of the mixed solution is adjusted by HNO_3 , rapid change in pH has influence on structure of the silica/RF composite and therefore the structure of silicon nitride as well. Comparing with the product from silica/RF composite without pH control (Figure 4.20), a decrease in macropore of the silicon nitride is observed when pH of the silica/RF solution is adjusted toward acidic. On the other hand, when compared with RF carbon (Figure 4.23d), the products with pH control have smaller mesopore. Products obtained from all values of pH are almost purely mesoporous. APTMS added to the RF solution results in a decrease in the mesopore diameter of the obtained silicon nitride product.

Figure 4.24 shows XRD analysis of products which were prepared by adjusting pH of the silica/RF solution at different values. It can be seen that the synthesis pH also influence the crystalline phase of the silicon nitride product. At pH 4.0 and 5.0

the obtained products consist of α -silicon nitride and small fraction of β -silicon nitride, but at pH 3.0, the product is amorphous. Table 4.3 shows surface area of silicon nitride powder synthesized with various pH values after calcination and RF carbon composite. The highest surface area obtain from silicon nitride prepared at pH = 4.0 while RF carbon composite and the others pH values are slightly difference surface area.

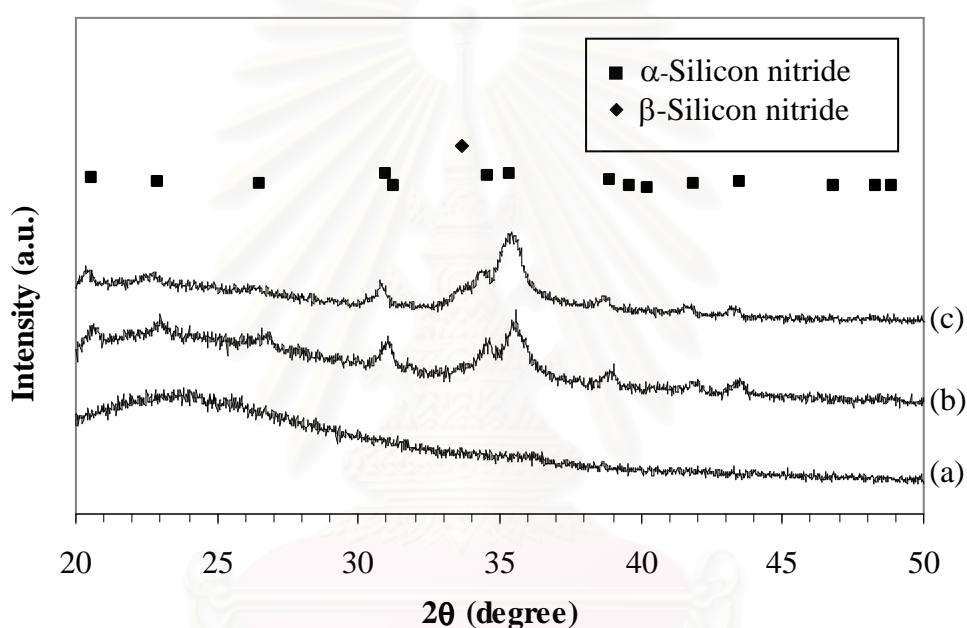


Figure 4.24 XRD patterns of the calcined silicon nitride powders prepared from silica/RF solution at different pH values: (a) pH = 3.0, (b) pH = 4.0 and (c) pH = 5.0.

Table 4.3 Surface area of calcined silicon nitride powder with Si/C ratio of 0.05, synthesized with various pH values, compared with RF carbon.

pH	Surface area (m ² /g)
3.0	381.72
4.0	549.19
5.0	343.52
7.4 *	334.29

* RF Carbon

TEM micrograph and SAED pattern in Figure 4.25 show amorphous phase in the sample synthesized at pH 3.0, which also confirm with XRD analysis result in Figure 4.24(a). Silicon nitride synthesized at pH 4.0 and 5.0 are polycrystalline, as confirmed by the SAED patterns in Figure 4.26(b) and 4.27(c) respectively. Closer investigation of the TEM micrographs reveals that single crystals of silicon nitride are agglomerated to form polycrystalline particles, as seen in Figure 4.26(a) and 4.27(a).

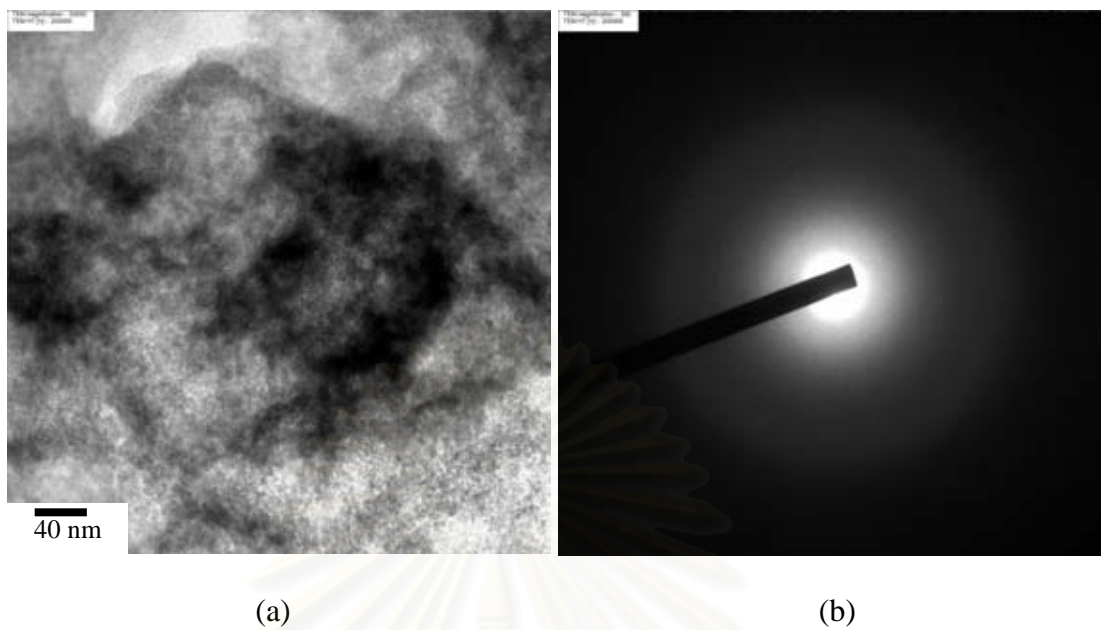


Figure 4.25 TEM micrograph and SAED pattern of the powder synthesized with Si/C molar ratio = 0.05 at pH 3.0, after calcination process.

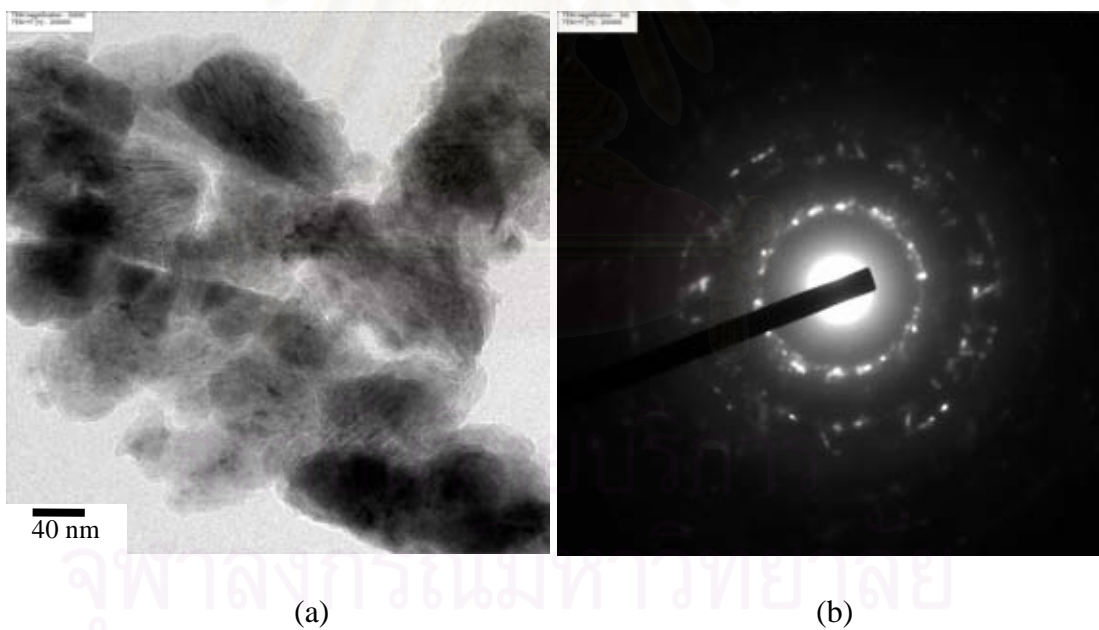
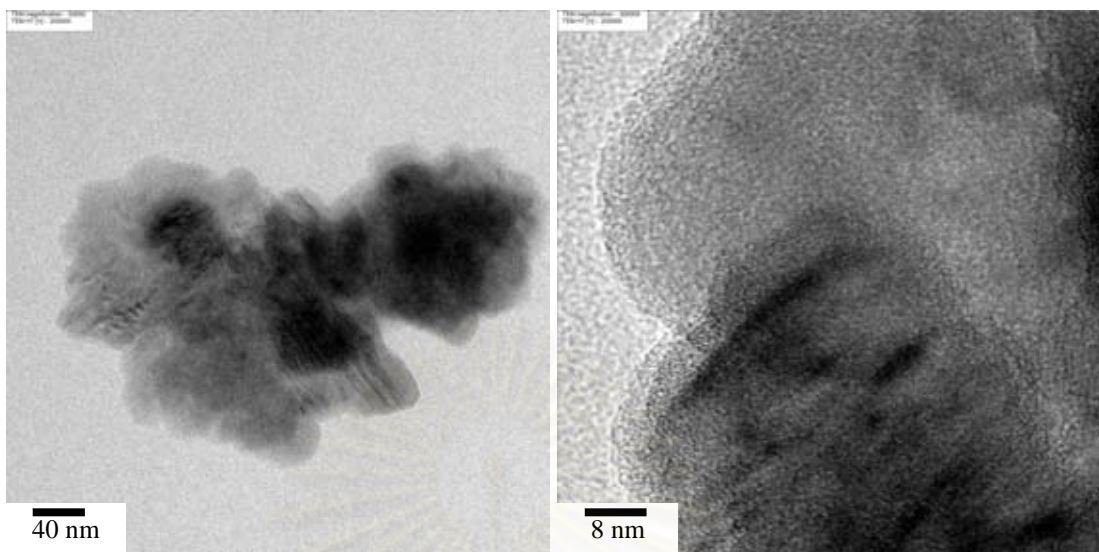
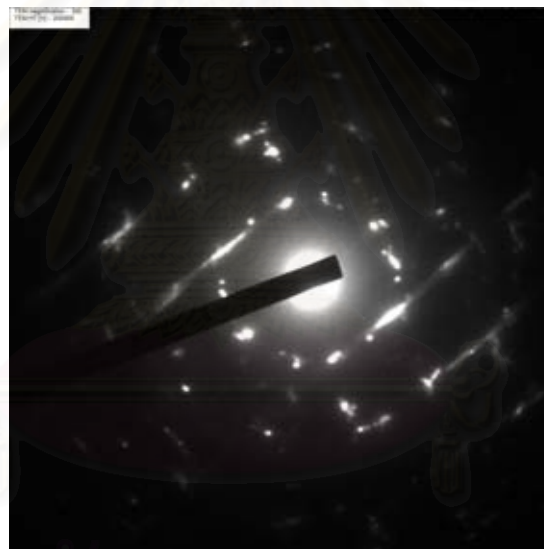


Figure 4.26 TEM micrograph and SAED pattern of the silicon nitride powder synthesized with Si/C molar ratio = 0.05 at pH 4.0, after calcination process.



(a)

(b)



(c)

Figure 4.27 TEM micrographs and SAED patterns of the silicon nitride powder synthesized with Si/C molar ratio = 0.05 at pH 5.0, after calcination process.

4.7 Effect of Reaction Time on Properties of Silicon Nitride

In this section, effect of reaction time during the carbothermal reduction and nitridation process is investigated. The reaction time investigated is in the range of 6-10 h. The silica/RF composites used in this section were prepared with Si/C ratio 0.05 and 0.07 without adjusting pH of the silica/RF solution. They were aged for 7 days, solvent exchanged with *t*-butanol and subsequently dried before pyrolyzed. The X-ray diffraction analysis results of products from the nitridation with different reaction time are shown in Figure 4.28 and 4.29.

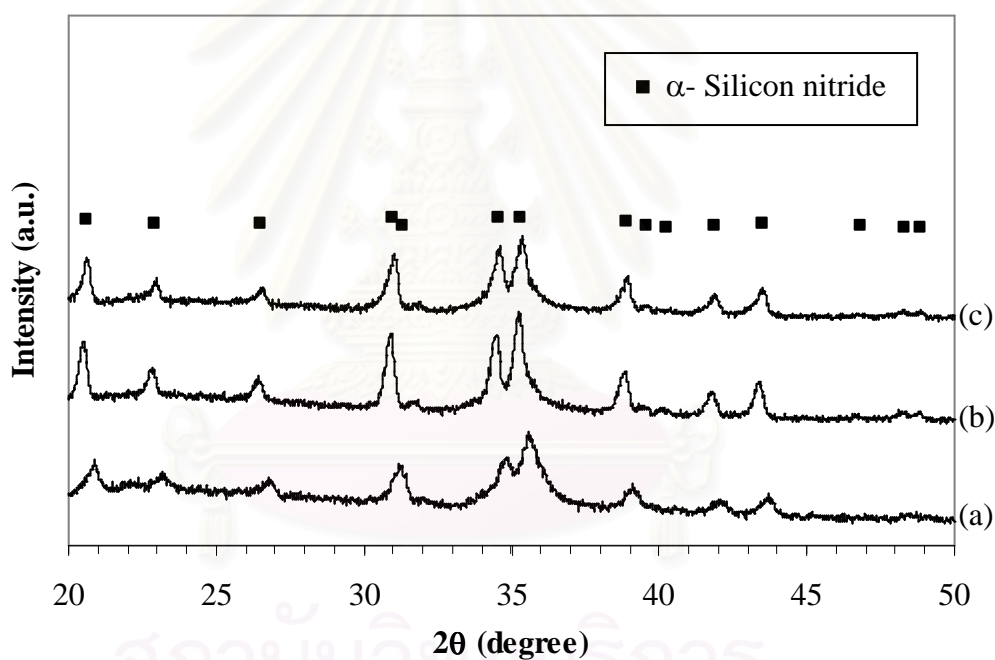


Figure 4.28 XRD patterns of products from the carbothermal reduction and nitridation of silica/RF composite at molar ratio Si/C=0.05 with various reaction times: (a) 6 h, (b) 8 h and (c) 10 h.

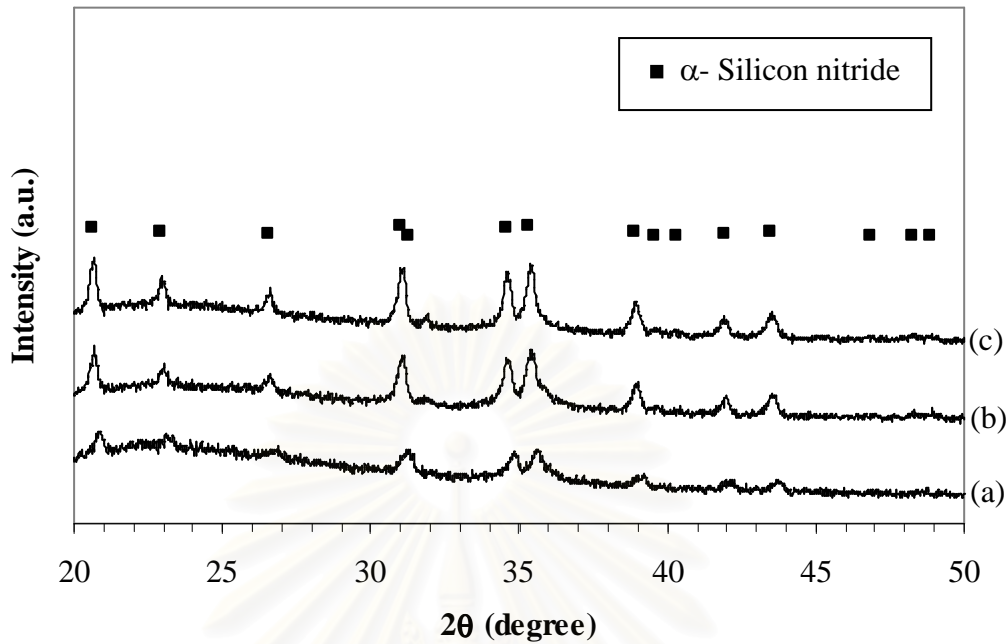
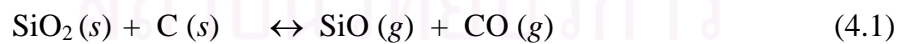


Figure 4.29 XRD patterns of products from the carbothermal reduction and nitridation of silica/RF composite at molar ratio Si/C=0.07 with various reaction times: (a) 6 h, (b) 8 h and (c) 10 h.

According to XRD patterns in Figure 4.28 and 4.29, it can be found that all products are α -silicon nitride. The sample mass loss increases when the reaction time for the carbothermal reduction and nitridation is prolonged as shown in Table 4.4. This result is in agreement with mechanism of silicon nitride synthesis via the carbothermal reduction and nitridation process proposed earlier (Segal 1985):

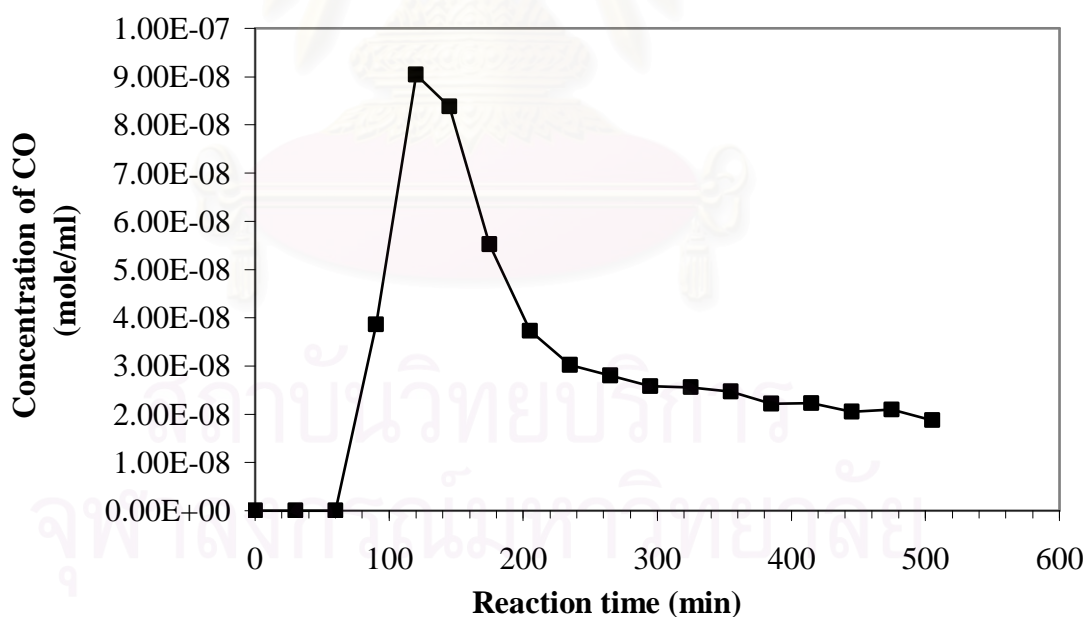


The longer the reaction time, more silicon monoxide is generated, according to Equation 4.1. Generation of silicon monoxide is responsible for mass loss in the sample.

Table 4.4 Sample mass loss after nitridation at various reaction times.

Molar ratio Si/C	Reaction time (h)	% mass loss	Average pore diameter (Å)	Surface area (m ² /g)
0.05	6	28.55	41.10	291.59
	8	33.70	45.13	328.58
	10	36.08	48.33	288.91
0.07	6	31.16	44.14	334.89
	8	37.44	46.27	354.92
	10	39.62	46.79	345.61

Table 4.4 also shows average pore size of the samples. The average pore diameter of the obtained silicon nitride powder increases as the reaction time is lengthen because the silicon nitride primary particles grow bigger, creating larger pores.

**Figure 4.30** Concentration of carbon monoxide gas which was generated during the carbothermal reduction and nitridation.

In this work, the concentration of carbon monoxide and carbon dioxide in the exhaust gas from the reaction were constantly monitored. No carbon dioxide was detected for the whole reaction process. For carbon monoxide, the results are shown in Figure 4.30. It should be noted that the time of 0 min in Figure 4.30 refers to the time which the system starts heating up from room temperature under constant flow of argon. It took 145 min for this heating up process, in which no reaction was taken place. Nitrogen gas was fed to the system after $t = 145$ min. According to Figure 4.30, when the temperature of the system reaches $900\text{ }^{\circ}\text{C}$ (at $t = 90$ min.), silica spontaneously reacts with carbon to generate silicon monoxide and carbon monoxide. The highest amount of carbon monoxide is generated at $1200\text{ }^{\circ}\text{C}$ ($t = 120$ min.). After nitrogen is supplied to the reactor, silicon monoxide gas reacts with carbon and nitrogen, according to Equation 4.2, resulting in silicon nitride and carbon monoxide. The concentration of carbon monoxide decreases as the reaction progresses, since silica in the silica/carbon composite is consumed. The overall reactions producing silicon nitride are shown in Equation 2.1.

Figure 4.31(a) and 4.32(a) show TEM micrographs of the silicon nitride powder synthesized after calcination process with Si/C molar ratio = 0.05 in the carbothermal reduction and nitridation for 8 h and 10 h respectively. The particles of silicon nitride in these figures are agglomerated. Figure 4.31(b) and 4.32(b) show morphology of silicon nitride particles. These results indicate that silicon nitride particles have many fine pores in the structure. Figure 4.31(c) and 4.32(c) indicate that when the carbothermal reduction and nitridation is prolonged, fine particles of silicon nitride agglomerate and sinter into polycrystalline particles. Silicon nitride in Figure 4.31(b) has lattice spacing of 0.208 nm.

The reaction time for the carbothermal reduction and nitridation also has the same effect on silicon nitride powder synthesized with Si/C molar ratio of 0.07. Figure 4.33(a) and 4.34(a) show that, as the reaction progresses (e.g. 8 or 10 h of reaction), particles of silicon nitride become more agglomerated than the silicon nitride synthesized for 6 h shown in Figure 4.19(a). SEAD patterns in Figure 4.33(c) and 4.34(c) also show that the obtained silicon nitrides are polycrystalline.

Silicon nitrides synthesized via the carbothermal reduction and nitridation for 8 and 10 h with this Si/C molar ratio have lattice spacing of 0.226 nm and 0.205 nm respectively.

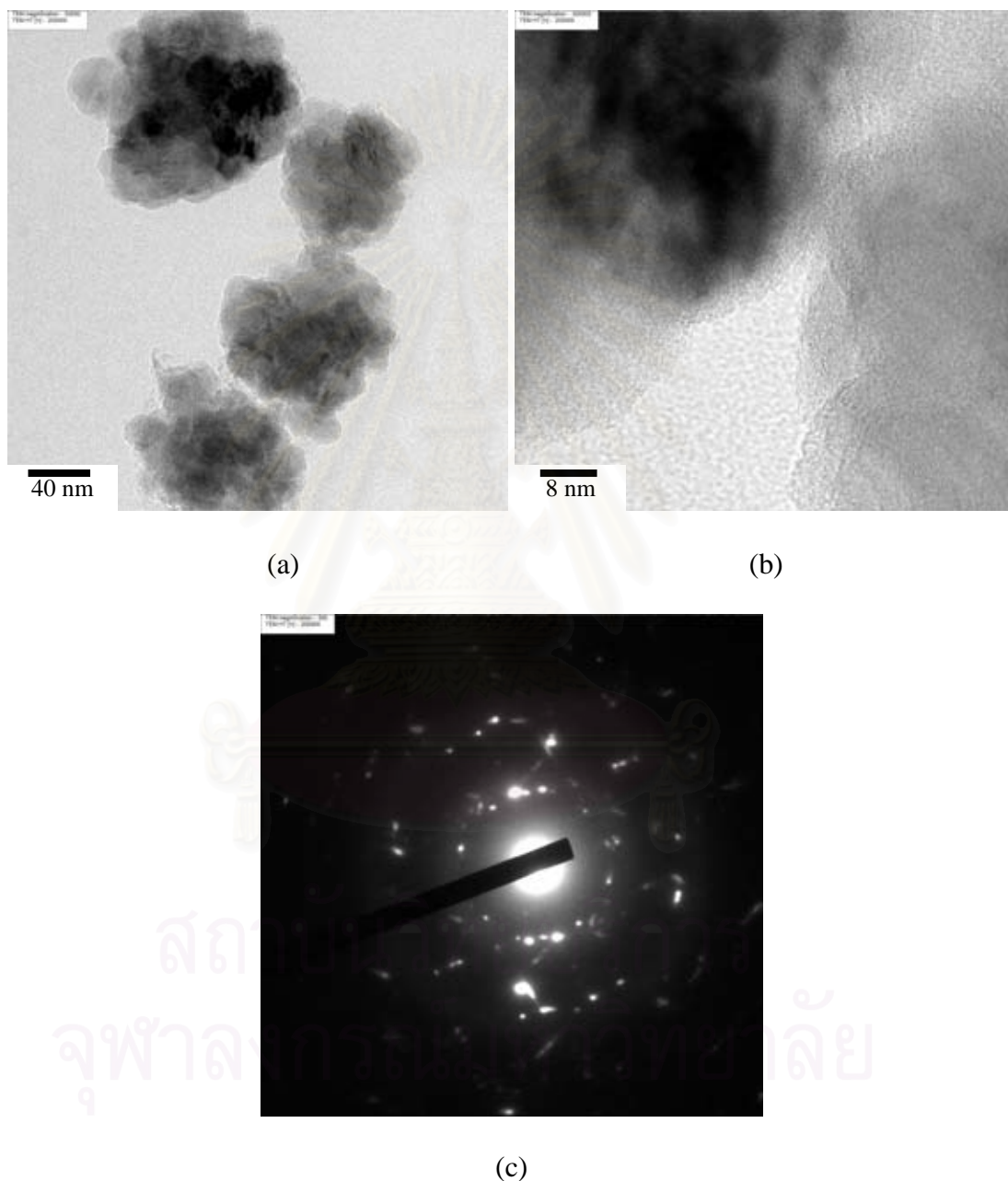


Figure 4.31 TEM micrograph and SAED pattern of the silicon nitride powder with Si/C molar ratio = 0.05 synthesized via the carbothermal reduction and nitridation for 8 h, after calcination process.

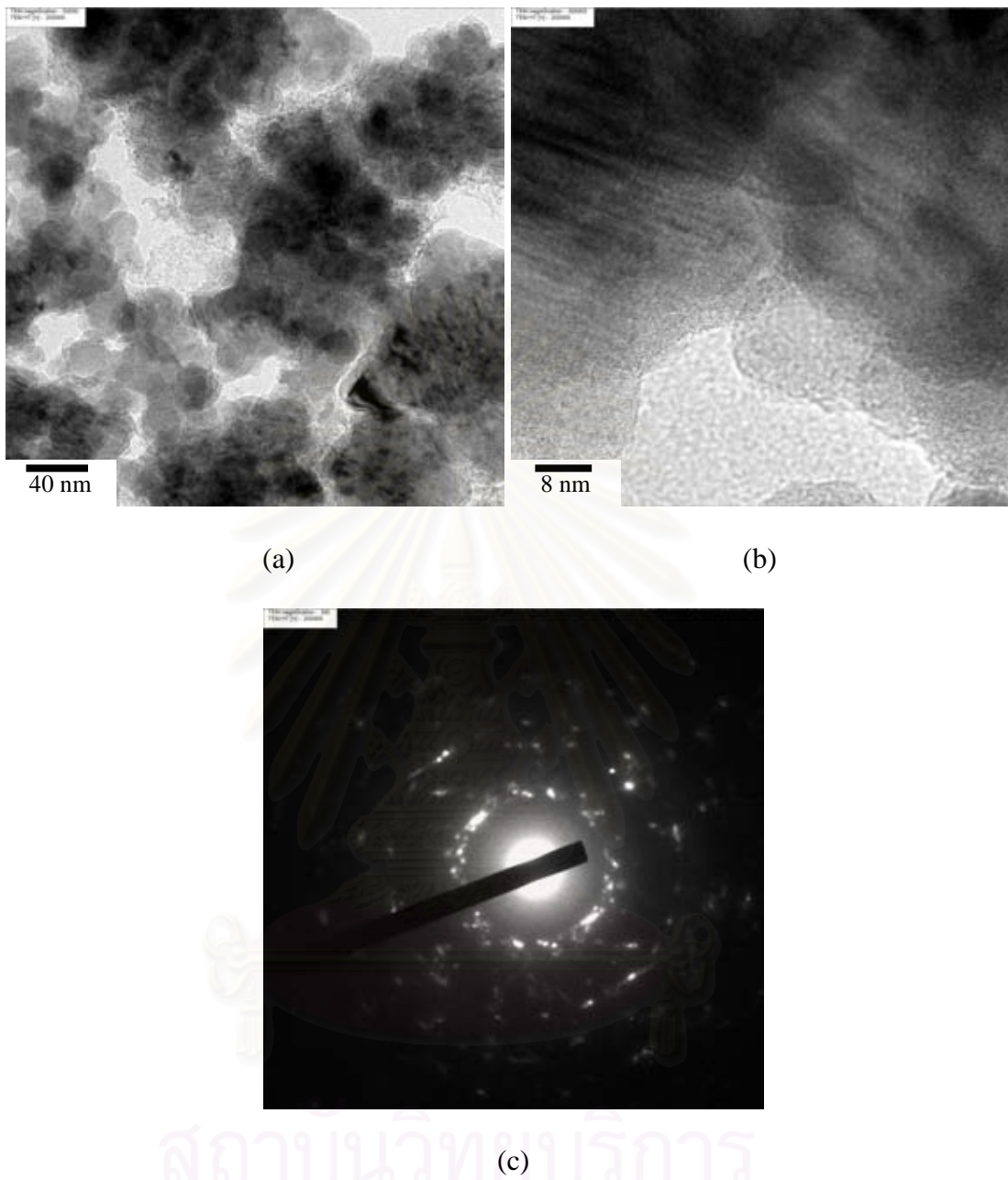


Figure 4.32 TEM micrograph and SAED pattern of the silicon nitride powder with Si/C molar ratio = 0.05 synthesized via the carbothermal reduction and nitridation for 10 h, after calcination process.

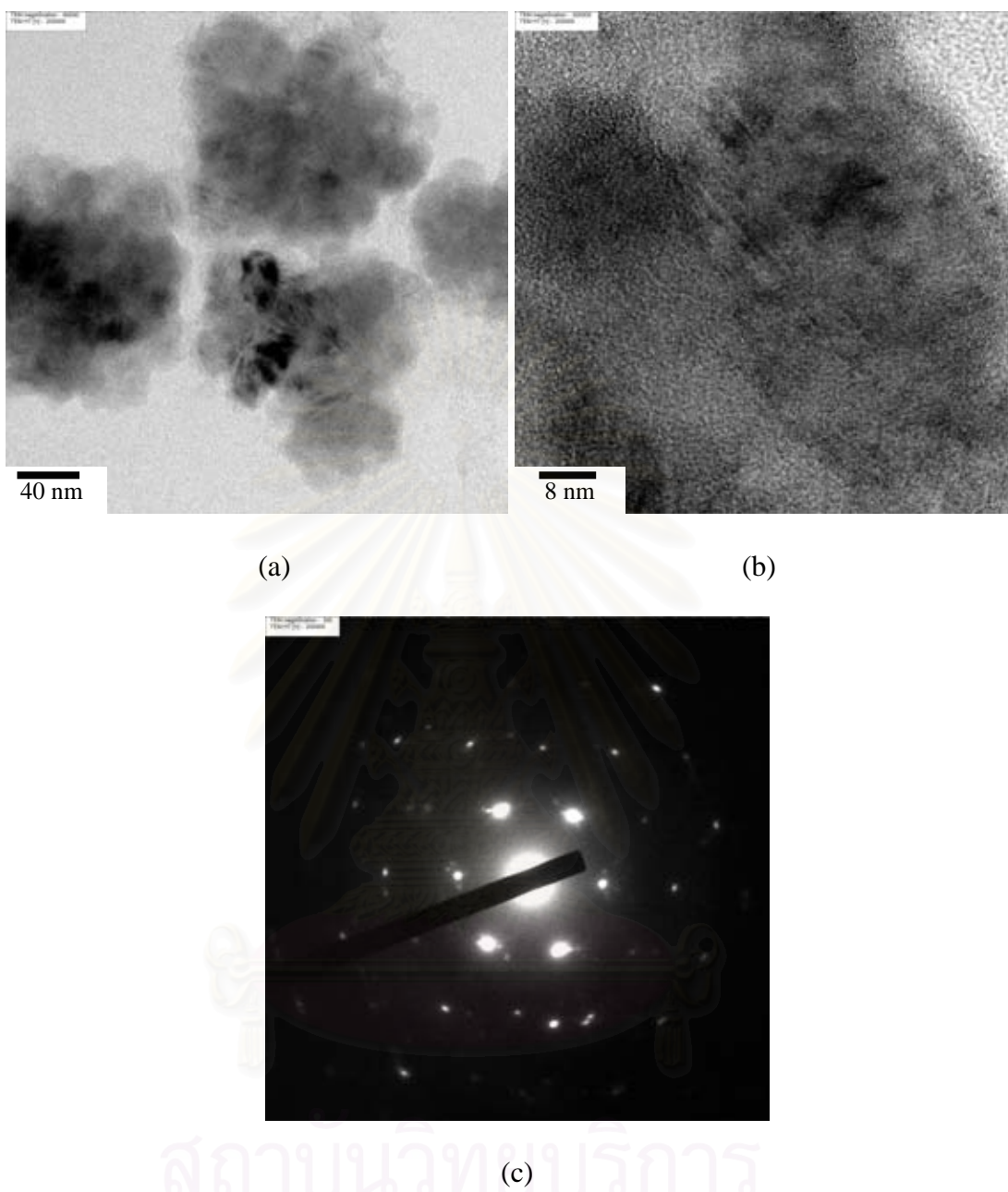


Figure 4.33 TEM micrograph and SAED pattern of the silicon nitride powder with Si/C molar ratio = 0.07 synthesized via the carbothermal reduction and nitridation for 8 h, after calcination process.

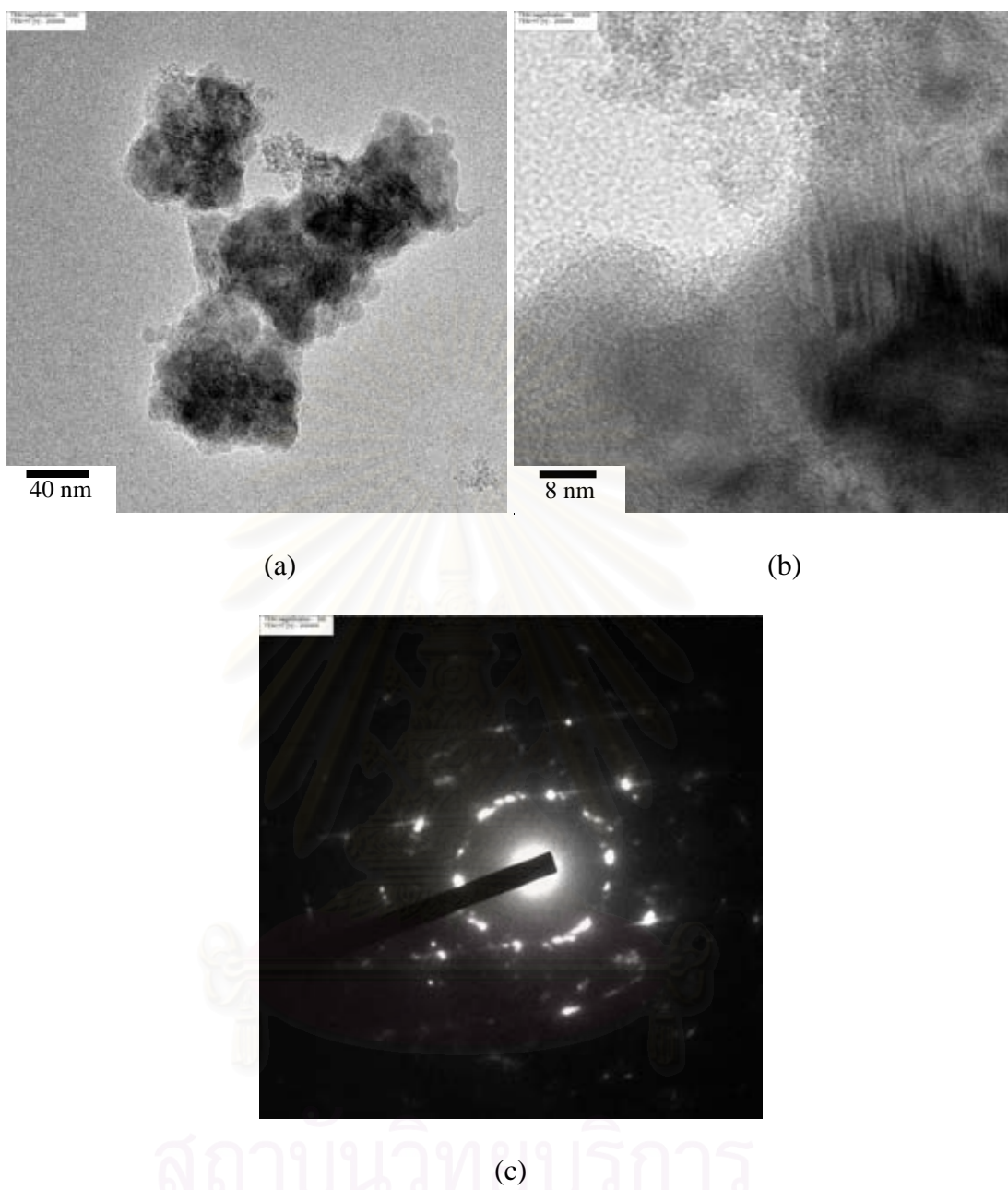


Figure 4.34 TEM micrograph and SAED pattern of the silicon nitride powder with Si/C molar ratio = 0.07 synthesized via the carbothermal reduction and nitridation for 10 h, after calcination process.

CHAPTER V

CONCLUSIONS AND RECOMMENDATION

5.1 Conclusions

In this work, preparation of silica/RF gel composite and the reaction to convert the composite into porous silicon nitride were investigated. The conclusions of the present research are the following:

1. Porous silicon nitride was successfully synthesized from silica/RF gel composite via the carbothermal reduction and nitridation. All silicon nitride products synthesized in this work are mainly in α -phase and have much higher surface area than the conventional silicon nitride granules, which indicates significant increase in porosity.
2. APTMS is a suitable precursor of silica in the synthesis of silicon nitride from the silica/RF composite. It has suitable structure to form crosslinked Si-O-Si network which can produce silicon nitride during the carbothermal reduction and nitridation.
3. Molar ratio of silicon and carbon has influence on surface area of silicon nitride product. Lower Si-to-C ratio gives silicon nitride powder which has low surface area. Higher the Si/C ratio leads to the stronger pore structure and high surface area.
4. Solvent exchange and aging of gel are an effective way to prevent the collapse of pore structures. Removal water in pore of the gel with *t*-butanol avoids shrinkage or crack of the network in the gel body. The strong pore structure which is formed during long aging period of gel can withstand the temperature of the synthesis.

5.2 Recommendations for Future Work

Synthesis of porous silicon nitride from silica/RF gel composite via the carbothermal reduction and nitridation process as well as effects of various factors, such as type of silica precursor, the molar ratio of silicon and carbon, aging time, solvent exchange of the obtained gel and reaction time, on yield of silicon nitride have been investigated in this work. Some recommendations for future work are listed as follows:

- (1) Porosity of the obtained silicon nitride should be measured by mercury absorption technique.
- (2) Formation of silica/RF gels in shaped articles should be further investigated. Silicon nitride in such form can be tested on strength, toughness and conductivity. It is also easy to use in many applications.

REFERENCES

- Aguado-Serrano, J., Rojas-Cervantes, M.L., Lo'pez-Peinado, A.J., and Go'mez-Serrano, V. (2004). "Silica/C Composites Prepared by the Sol-Gel Method. Influence of the Synthesis Parameters on Textural Characteristics." *Microporous and mesoporous materials* 74: 111-119.
- Cheng, F., Clark, S., Kelly, S.M., Bradley, J.S., and Lefebvre, F. (2004). "Preparation of Mesoporous Silicon Nitride via a Nonaqueous Sol-Gel Route." *Journal of the American Ceramic Society* 87(8): 1413-1417.
- Czakkel, O., Marthi, K., Geissler, E., and La'szlo', K. (2005). "Influence of Drying on the Morphology of Resorcinol-Formaldehyde-Based Carbon Gels." *Microporous and Mesoporous Materials* 86: 124-133.
- Liu, D.M. (1997). "Fabrication of Hydroxyapatite Ceramic with Controlled Porosity." *Journal of Materials Sciences* 8: 227-232.
- Di'az, A., Hampshire, S., Yang, J.-F., Ohji, T., and Kanzaki, S. (2005). "Comparison of Mechanical Properties of Silicon Nitrides with Controlled Porosities Produced by Different Fabrication Routes." *Journal of the American Ceramic Society* 88(3): 698-706.
- Di'az, A., and Hampshire, S. (2004). "Characterisation of Porous Silicon Nitride Materials Produced with Starch." *Journal of the European Ceramic Society* 24: 413-419.
- Husing, N., and Schubert, U. (2005). "Aerogels." *Institut für Anorganische Chemie, Technische Universität Wien, A-1060 Wien, Austria*, 1-27.
- Inagaki, Y., Ohji, T., Kanzaki, S., and Shigegaki, Y. (2000). "Fracture Energy of an Aligned Porous Silicon Nitride." *Journal of the American Ceramic Society* 83(7): 1807-1809.

- Kamiya, K., Sano, T.Y.T., and Tanaka, K. (1990). "Distribution of Carbon Particles in Carbon/SiO₂ Glass Composites Made from CH₃Si(OC₂H₅)₃ by the Sol-Gel Method." *Journal of Non-Crystalline Solids* 119: 14-20.
- Karmakar, B., De, G., and Ganguli, D. (2000). "Dense Silica Microspheres from Organic and Inorganic Acid Hydrolysis of TEOS." *Journal of Non-Crystalline Solids* 272: 119-126.
- Kaskel, S., and Schlichte, K. (2001). "Porous Silicon Nitride as a Superbase Catalyst." *Journal of Catalysis* 201: 270-274.
- Kawai, C., and Yamakawa, A. (1998). "Crystal Growth of Silicon Nitride Whiskers Through a VLS Mechanism Using SiO₂-Al₂O₃-Y₂O₃ Oxides as Liquid Phase." *Ceramics International* 24: 136-138.
- Kawai, C., and Yamakawa, A. (1997). "Effect of Porosity and Microstructure on the Strength of Si₃N₄: Designed Microstructure for High Strength, High Thermal Shock Resistance, and Facile Machining." *Journal of the American Ceramic Society* 80(10): 2705-2708.
- Kondo, N., Inagaki, Y., Suzuki, Y., and Ohji, T. (2002). "Fabrication of Porous Anisotropic Silicon Nitride by Using Partial Sinter-Forging Technique." *Materials Science and Engineering A* 335: 26-31.
- Lin, C., and Ritter, J.A. (1997). "Effect of Synthesis pH on the Structure of Carbon Xerogels." *Carbon* 35(9): 1271-1278.
- Lyckfeldt, O., and Ferreira, J.M.F. (1998). "Processing of Porous Ceramics by Starch Consolidation." *Journal of the European Ceramic Society* 18: 131-140.

- Matovic, B. (2003). "Low Temperature Sintering Additives for Silicon Nitride." *Max-Planck-Institut für Metallforschung Stuttgart*: 1-133.
- Pekala, R.W. (1989). "Organic Aerogels from the Polycondensation of Resorcinol with Formaldehyde." *Journal of Materials Science* 24: 3221-3227.
- Riley, F.L. (2000). "Silicon Nitride and Related Materials." *Journal of the American Ceramic Society* 83(2): 245-265.
- Segal, D.L. (1985). "Developments in the Synthesis of Silicon Nitride." *Chemistry and Industry* 16: 544-545.
- Suttor, D.S., and Fischman, G.S. (1992). "Densification and Sintering Kinetics in Sintered Silicon Nitride." *Journal of the American Ceramic Society* 75(5): 1063-1067.
- Tamon, H., Ishizaka, H., Yamamoto, T., and Suzuki, T. (1999). "Preparation of Mesoporous Carbon by Freeze Drying." *Carbon* 37: 2049-2055.
- Tonanon, N., Siyasukh, A., Tanthapanichakoon, W., Nishihara, H., Mukai, S.R., and Tamon, H. (2005). "Improvement of Mesoporosity of Carbon Cryogels by Ultrasonic Irradiation." *Carbon* 43: 525-531.
- Trassl, S., Kleebe, H.-J., Stoßner, H., Motz, G., Rossler, E., and Ziegler, G. (2002). "Characterization of the Free-Carbon Phase in Si-C-N Ceramics: Part II, Comparison of Different Polysilazane Precursors." *Journal of the American Ceramic Society* 85(5): 1268-1274.
- Turkdogan, E.T., Bills, P.M., and Tippett, V.A. (1958). "Silicon Nitrides: Some Physico-Chemical Properties." *Journal of Apply Chemistry* 8: 296-302.

- Wiener, M., Reichenauer, G., Scherb, T., and Fricke, J. (2004). "Accelerating the Synthesis of Carbon Aerogel Precursors." *Journal of Non-Crystalline Solids* 350: 126-130.
- Yang, J.-F., Ohji, T., Kanzaki, S., Diaz, A., and Hampshire, S. (2002). "Microstructure and Mechanical Properties of Silicon Nitride Ceramics with Controlled Porosity." *Journal of the American Ceramic Society* 85(6): 1512-1516.
- Yang, J.-F., Shan, S.-Y., Janssen, R., Schneider, G., Ohji, T., and Kanzaki, S. (2005a). "Synthesis of Fibrous β -Si₃N₄ Structured Porous Ceramics Using Carbothermal Nitridation of Silica." *Acta Materialia* 53: 2981-2990.
- Yang, J.-F., Zhang, G.-J., Kondo, N., Ohji, T., and Kanzaki, S. (2005b). "Synthesis of Porous Si₃N₄ Ceramics with Rod-Shaped Pore Structure." *Journal of the American Ceramic Society* 88(4): 1030-1032.
- Yang, J.-F., Zhang, G.-J., Kondo, N., She, J.-H., Jin, Z.-H., Ohji, T., and Kanzaki, S. (2003). "Porous 2H-Silicon Carbide Ceramics Fabricated by Carbothermal Reaction Between Silicon Nitride and Carbon." *Journal of the American Ceramic Society* 86(6): 910-914.
- Yang, J.-F., Zhang, G.-J., and Ohji, T. (2001). "Fabrication of Low-Shrinkage, Porous Silicon Nitride Ceramics by Addition of a Small Amount of Carbon." *Journal of the American Ceramic Society* 84(7): 1639-1641.
- Yang, J. F., Ohji, T., and Niihara, K. (2000). "The Influence of Y₂O₃-Al₂O₃ Content on Sintering Process and Microstructure of Silicon Nitride Ceramics." *Journal of the American Ceramic Society* 83(8): 2094-2096.

Zhang, W., Wang, H., and Jin, Z. (2005). "Gel Casting and Properties of Porous Silicon Carbide/Silicon Nitride Composite Ceramics." *Materials Letters* 59: 250-256.

Zhang, G.-J., Yang, J.-F., Deng, Z.Y., and Ohji, T. (2001). "Fabrication of Porous Ceramics with Unidirectionally Aligned Continuous Pores." *Journal of the American Ceramic Society* 84: 1395-1397.



สถาบันวิทยบริการ
จุฬาลงกรณ์มหาวิทยาลัย

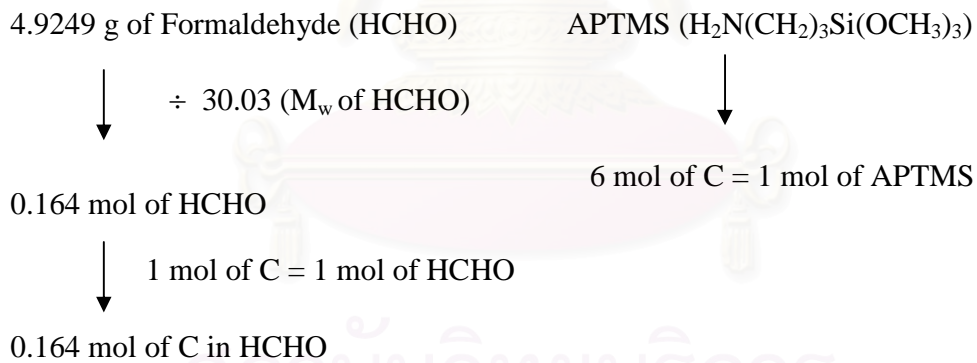
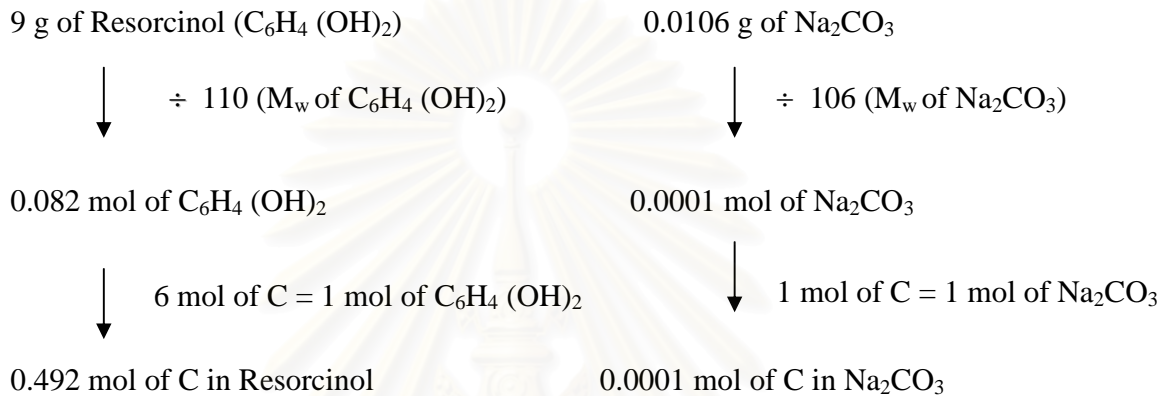


APPENDICES

สถาบันวิทยบริการ
จุฬาลงกรณ์มหาวิทยาลัย

APPENDIX A

CALCULATION OF MOLAR RATIO OF SILICON AND CARBON IN RF GEL COMPOSITE



↓
Mole of Si = Mole of APTMS

Molar ratio of carbon and silicon =

$$\frac{\text{Mole of Si in APTMS}}{\text{Mole of C in Resorcinol} + \text{Mole of C in HCHO} + \text{Mole of C in Na}_2\text{CO}_3 + \text{Mole of C in APTMS}}$$

$$\text{Molar ratio of carbon and silicon} = \frac{\text{Mole of APTMS}}{0.492 + 0.164 + 0.0001 + 6(\text{Mole of APTMS})}$$

For example, Molar ratio of carbon and silicon = 0.03

$$\text{From calculation, } 0.03 = \frac{\text{Mole of APTMS}}{0.492 + 0.164 + 0.0001 + 6(\text{Mole of APTMS})}$$

$$\begin{aligned} \text{Get, Mole of APTMS} &= 0.024 \\ &= 4.2984 \text{ g of APTMS} \end{aligned}$$

สถาบันวิทยบริการ
จุฬาลงกรณ์มหาวิทยาลัย

APPENDIX B

DATA OF PORE DIAMETER AND PORE VOLUME

Table B.1 Data of pore diameter and pore volume of calcined sample with molar ratio of Si/C = 0.05, synthesized with solvent exchange and no aging.

Pore Diameter (Å)	Pore Volume (cm ³ /g)
730.5246759	0.017709103
454.2057471	0.076979252
309.3363368	0.108904575
236.4831626	0.121776221
150.3452867	0.123451022
92.33689923	0.151619497
51.75581891	0.282081581
31.89212644	0.457763573
19.52373432	0.161067956

Table B.2 Data of pore diameter and pore volume of calcined sample with molar ratio of Si/C = 0.05, synthesized with solvent exchange and aged for 1 day.

Pore Diameter (Å)	Pore Volume (cm ³ /g)
736.4002045	0.030494918
452.5800288	0.098404066
305.5532602	0.115241196
236.2304413	0.139076584
149.6355734	0.103773981
86.94097688	0.142025834
51.09384972	0.300890504
31.66545068	0.501052096
18.41003190	0.141807296

Table B.3 Data of pore diameter and pore volume of calcined sample with molar ratio of Si/C = 0.05, synthesized with solvent exchange and aged for 3 days.

Pore Diameter (Å)	Pore Volume (cm ³ /g)
746.4707951	0.007459517
467.5466233	0.050960069
315.6449947	0.068547619
240.3404764	0.080323804
152.2355867	0.093796511
92.74465255	0.152231703
49.92679533	0.564500284
31.37919738	0.897563590
19.30344892	0.314300235

Table B.4 Data of pore diameter and pore volume of calcined sample with molar ratio of Si/C = 0.05, synthesized with solvent exchange and aged for 5 days.

Pore Diameter (Å)	Pore Volume (cm ³ /g)
736.8325160	0.015929782
458.5152987	0.063656623
311.1054599	0.085400583
236.7232933	0.104144317
150.3261052	0.109304694
91.82105703	0.132191321
51.18063611	0.365249516
31.26938355	0.479866510
19.01167130	0.133219180

Table B.5 Data of pore diameter and pore volume of calcined sample with molar ratio of Si/C = 0.05, synthesized with solvent exchange and aged for 7 days.

Pore Diameter (Å)	Pore Volume (cm ³ /g)
704.4759749	0.013218245
433.9778379	0.038413888
298.0788614	0.059305099
234.0969676	0.096220772
150.3511411	0.101873655
91.23169779	0.183990712
49.93311625	0.618395072
30.51595158	0.661267659
18.28317282	0.164555530

Table B.6 Data of pore diameter and pore volume of calcined sample with molar ratio of Si/C = 0.07, synthesized with solvent exchange and no aging.

Pore Diameter (Å)	Pore Volume (cm ³ /g)
689.7639115	0.004958318
443.2900463	0.048633920
309.4913891	0.115122974
233.6613597	0.189135001
145.3361023	0.264860059
88.05171187	0.251781963
50.43344557	0.569611448
30.54319232	0.508101618
18.46193360	0.098900561

Table B.7 Data of pore diameter and pore volume of calcined sample with molar ratio of Si/C = 0.07, synthesized with solvent exchange and aged for 1 day.

Pore Diameter (Å)	Pore Volume (cm ³ /g)
670.2122202	0.001342049
436.9630201	0.055071750
310.5909780	0.131494165
231.7027929	0.202164931
152.0882416	0.251731676
90.85409686	0.285123655
50.35256169	0.564830514
31.41233267	0.610668490
19.38074951	0.163575411

Table B.8 Data of pore diameter and pore volume of calcined sample with molar ratio of Si/C = 0.07, synthesized with solvent exchange and aged for 3 days.

Pore Diameter (Å)	Pore Volume (cm ³ /g)
758.741200	0.013437394
500.7694032	0.081864033
327.2350032	0.130554668
238.2809147	0.173109943
151.6570541	0.222002839
91.22116588	0.297362624
49.50124195	0.649082749
30.89826784	0.642865218
18.88695573	0.146044410

Table B.9 Data of pore diameter and pore volume of calcined sample with molar ratio of Si/C = 0.07, synthesized with solvent exchange and aged for 5 days.

Pore Diameter (Å)	Pore Volume (cm ³ /g)
728.8077055	0.007072656
447.9084607	0.051578629
307.5088677	0.100689284
235.4893543	0.155183994
153.1048103	0.202480835
91.38938765	0.245754152
49.81397075	0.551918412
31.77046995	0.701023230
19.63394266	0.239846302

Table B.10 Data of pore diameter and pore volume of calcined sample with molar ratio of Si/C = 0.07, synthesized with solvent exchange and aged for 7 days.

Pore Diameter (Å)	Pore Volume (cm ³ /g)
711.1240400	0.052172854
443.8857376	0.152796312
301.6159798	0.161742370
233.8575924	0.178061442
148.8641438	0.098967332
84.83755821	0.082982313
47.66102872	0.188050143
29.24970035	0.348974959
17.17758795	0.034936342

APPENDIX C

CALIBRATION CURVES FOR QUANTITATIVE ANALYSIS BY GAS CHROMATOGRAPHY

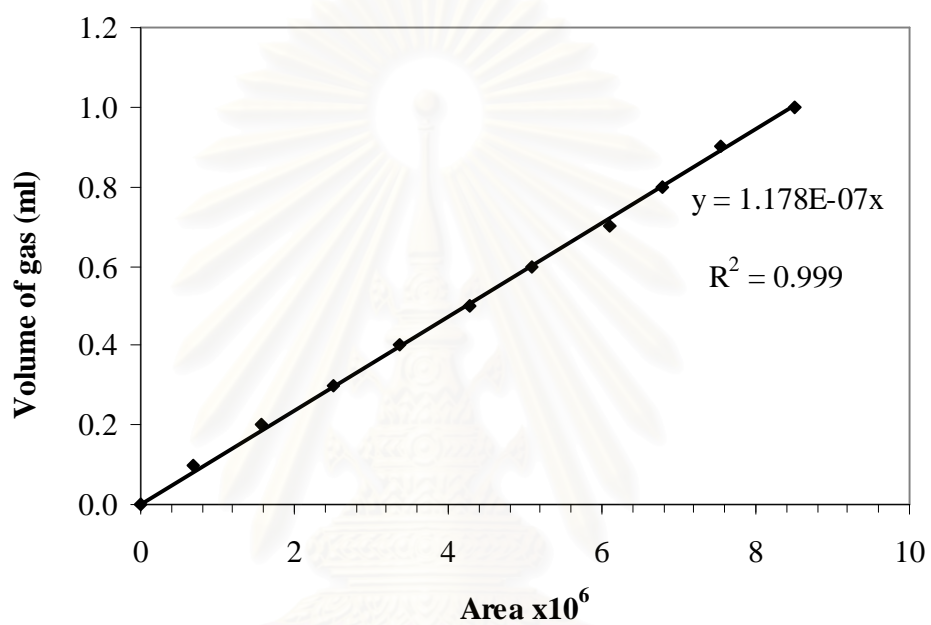


Figure C.1 The calibration curve for hydrogen

สถาบันวิทยบริการ
จุฬาลงกรณ์มหาวิทยาลัย

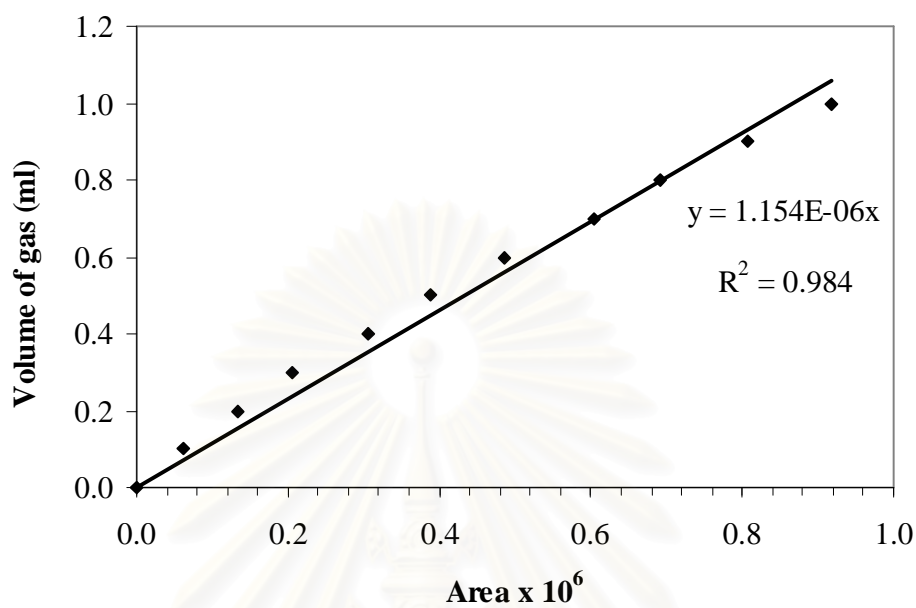


Figure C.2 The calibration curve for carbon monoxide

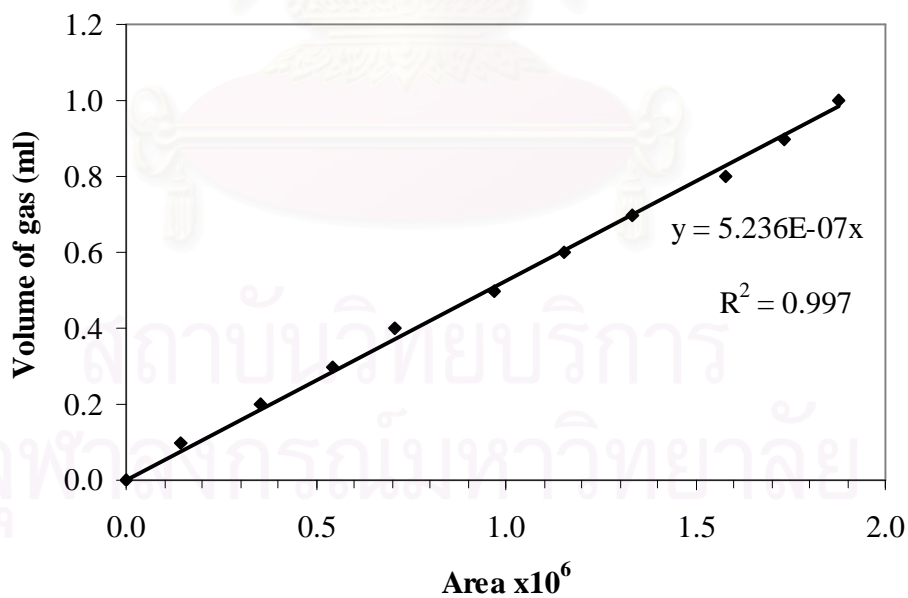


Figure C.3 The calibration curve for nitrogen

APPENDIX D

PICTURES OF SILICA/RF COMPOSITES

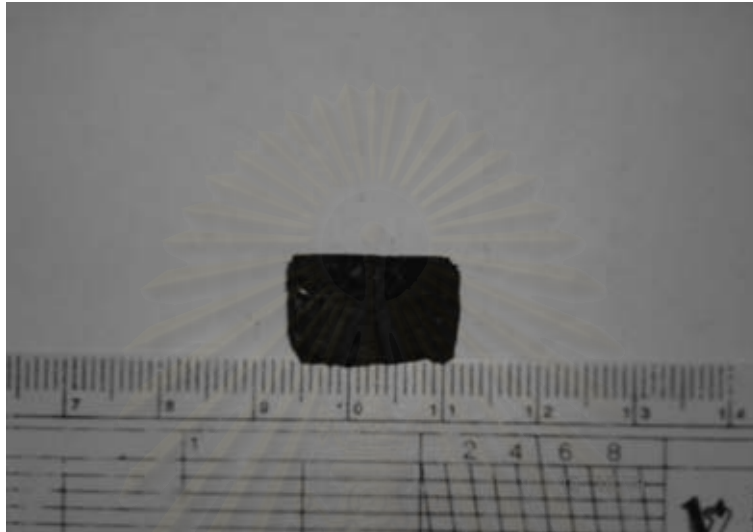


Figure D.1 Silica/RF composite obtained after pyrolysis process.

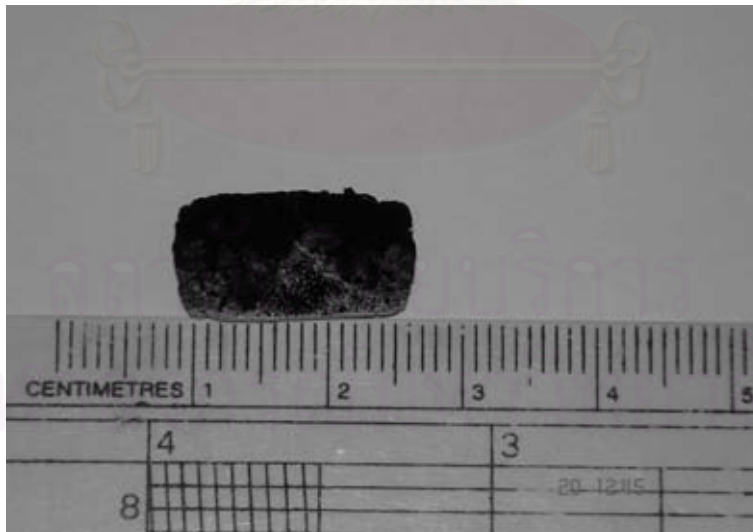


Figure D.2 Silica/RF composite obtained after the carbothermal reduction and nitridation.

APPENDIX E

SEM MICROGRAPHS OF SILICON NITRIDE POWDER SYTHESIZED AFTER CALCINATION PROCESS

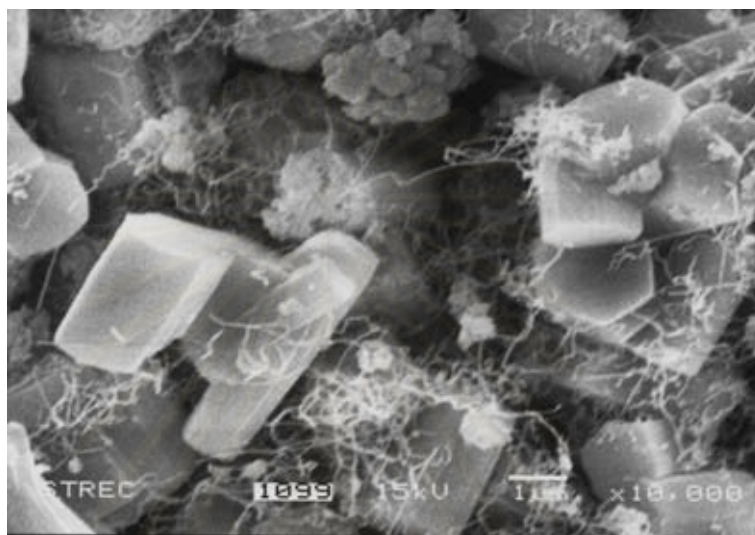


Figure E.1 SEM micrograph of silicon nitride powder with Si/C molar ratio of 0.02 prepared without solvent exchange after calcination process.

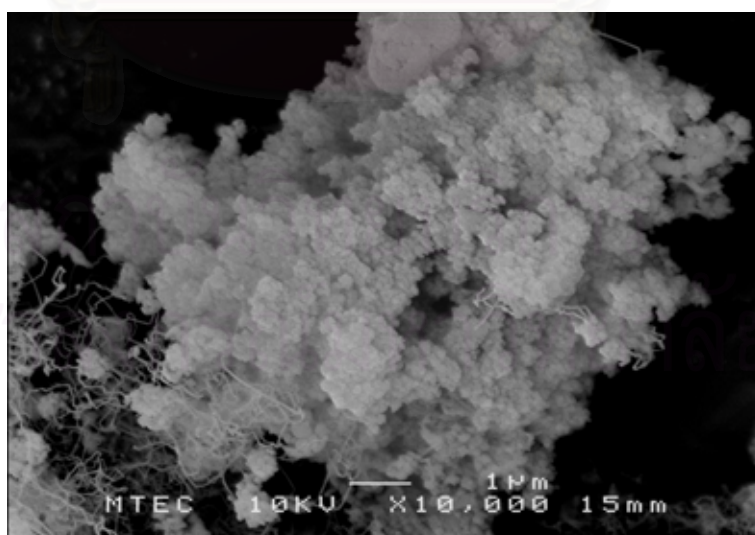


Figure E.2 SEM micrograph of silicon nitride powder with Si/C molar ratio of 0.07 prepared without solvent exchange after calcination process.

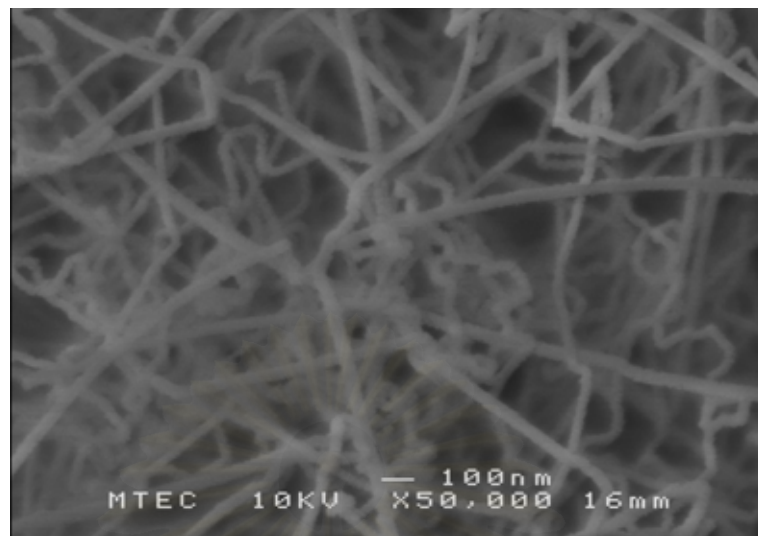


Figure E.3 SEM micrograph of silicon nitride powder with Si/C molar ratio of 0.07 prepared without solvent exchange after calcination process.

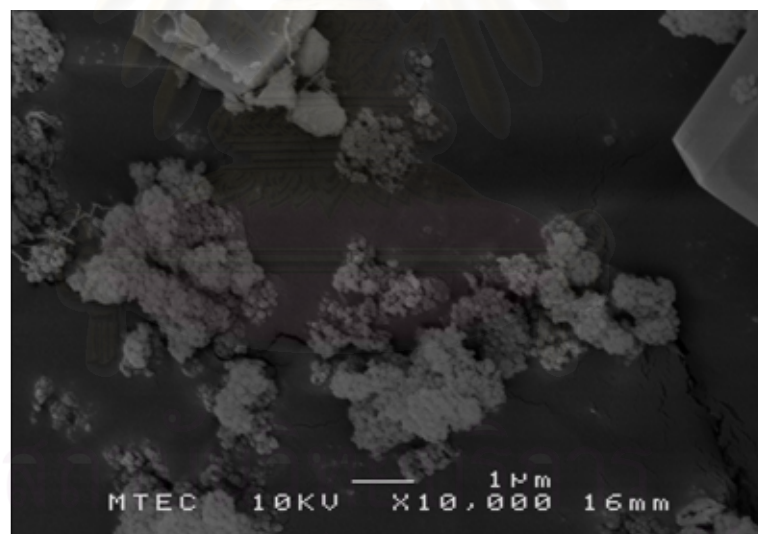


Figure E.4 SEM micrograph of silicon nitride powder with Si/C molar ratio of 0.07 prepared with solvent exchange after calcination process.

APPENDIX F

LIST OF PUBLICATION

1. Kanoksak Luyjew, Nattaporn Tonanon and Varong Pavarajarn “Porous Silicon Nitride Synthesis from the Carbothermal Reduction and Nitridation of Silica/RF Gel Composite”, Proceedings of the Regional Symposium on Chemical Engineering 2006, Nanyang , Singapore, December 3rd-5th, 2005.



สถาบันวิทยบริการ
จุฬาลงกรณ์มหาวิทยาลัย

Porous Silicon Nitride Synthesis from the Carbothermal Reduction and Nitridation of Silica/RF Gel Composite

Kanoksak Luyjew^a, Nattaporn Tonanon^b and Varong Pavarajarn^{a,*}

^a) Center of Excellence on Catalysis and Catalytic Reaction Engineering, Department of Chemical Engineering, Chulalongkorn University, Bangkok 10330, Thailand

^b) Center of Excellence on Particle Technology, Department of Chemical Engineering, Chulalongkorn University, Bangkok 10330, Thailand

* Corresponding author: Tel. +66-2-218-6890, Email: fchvpv@eng.chula.ac.th

ABSTRACT

Porous silicon nitride was synthesized by the carbothermal reduction and nitridation of silica/carbon composite prepared by carbonization of silica/RF gel composite. Various techniques such as X-ray diffraction (XRD), Fourier transform infrared spectroscopy (FTIR), Scanning electron microscopy (SEM), Thermogravimetric analysis (TGA) and surface area determination via nitrogen absorption (BET) were employed to characterize the obtained products. The obtained products contain α -silicon nitride as the major crystalline phase. Significant increase in surface area of the products, comparing to that of the conventional silicon nitride granules, was observed. The silicon-to-carbon molar ratio in the composite and method to remove water from the composite gel were the major factors influencing the porosity of the final product.

INTRODUCTION

Porous ceramics have been attracting great interest for various applications, such as filtration in severe environments and being light-weighted insulator. However, the main disadvantage of the porous material is its low strength. It is therefore the objective of this work to synthesize porous structure from high-strength ceramic, namely silicon nitride.

Silicon nitride (Si_3N_4) is a structural ceramic with good high-temperature property. It has been used for various applications that require high strength at elevated temperature. Silicon nitride can be synthesized by many techniques but the obtained silicon nitride powder usually has low porosity and low surface area. In this work, a novel technique to synthesize porous silicon nitride from the carbothermal and nitridation of silica/RF gel composite is presented.

MATERIALS AND METHODS

The silica/RF composite was first synthesized by co-polymerization of resorcinol–formaldehyde (RF) aqueous solution with amino propyl trimethoxysilane (APTMS). After aging at room temperature for predetermined period, water was removed from the composite by solvent exchange with *t*-butanol. The obtained product was dried at 110°C for 16 h and subjected to stepwise pyrolysis at 250°C for 2 h and at 750°C for 4 h in nitrogen to get silica/carbon composite. The conversion from silica/carbon composite to silicon nitride based on the carbothermal reduction and nitridation process was conducted at 1450°C for 6 h in nitrogen. Carbon residue in the product was removed by subsequent calcination at 700°C for 10 h. Various techniques, i.e. X-ray diffraction (XRD), Fourier transform infrared spectroscopy (FTIR), scanning electron microscopy (SEM), thermogravimetric analysis (TGA) and surface area determination via nitrogen absorption (BET), were employed to characterize the obtained products.

RESULTS AND DISCUSSION

The XRD analysis confirmed that the product obtained after the nitridation was silicon nitride, mainly in α -phase. No other crystalline phase was detected. It can be seen from Table 1 that all products synthesized in this work have much higher surface area than the conventional silicon nitride granules, which indicated significant increase in porosity. At low content of silicon, the surface area increased when amount of silica precursor was increased. The surface area of the product reached maximum at Si/C molar ratio in the silica/carbon composite of 0.05, at which the product was consisted of uniformly dispersed silicon nitride fine grains. Figure 1 shows SEM micrographs that clearly indicates the uniformity of grains as well as fine pores in the sample. The molar ratio higher than 0.05 resulted in

segregation of silica within the silica/carbon composite that yielded large silicon nitride grains and decreased surface area.

The results in Table 1 also show that the method to remove water from the silica/RF composite greatly affected the pore structure of the final product. The product that had been treated with *t*-butanol in the solvent exchange process had higher surface area than the product that was dried without solvent exchange. Since water has high surface tension, removal of water from a pore by direct drying can cause the pore structure to collapse. On the other hand, water removal by exchanging with *t*-butanol, before subsequently drying, can prevent such effect because *t*-butanol has lower surface tension.

Table 1. Surface area of Silicon nitride powder at various molar ratio of Si/C.

Si/C molar ratio	Surface area (m ² /g)	
	with solvent exchange	without solvent exchange
0.01	69.57	60.95
0.02	74.64	62.00
0.03	263.88	161.21
0.05	267.80	239.21
0.07	99.14	78.73
Commercial silicon nitride*	1.2-13.0	

* source: PRED Materials international, Inc.

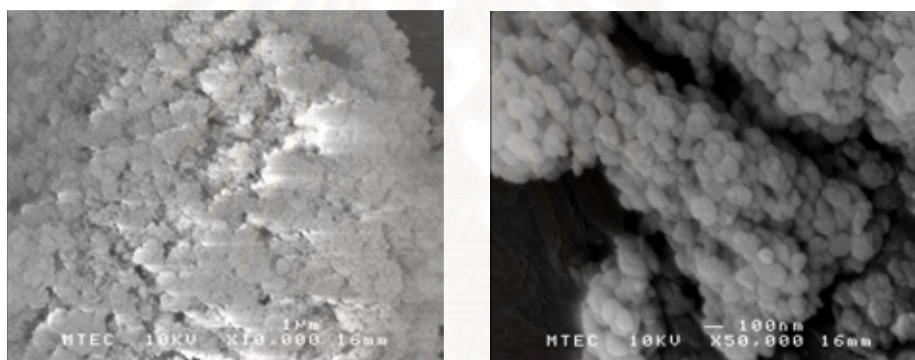


Figure 1. Microstructure of silicon nitride product with Si/C molar ratio of 0.07

The thermogravimetric analysis of the final products by heating the sample in oxygen revealed no significant mass decrease, which confirmed that no carbon was remained in the product after the calcination. Instead, slight mass increase was observed at the analysis temperature higher than 700°C. This is the result from surface oxidation of silicon nitride.

CONCLUSION

Porous silicon nitride powder can be synthesized via the carbothermal reduction and nitridation of silica/carbon composite. Pore structure of the final product can be controlled from the structure of the silica/RF composite, which is the starting material. The silica-to-carbon ratio of the starting composite influences size of the silicon nitride grains obtained, which consequently affects the porosity of the product. Optimum Si/C molar ratio of 0.05 was found to result in silicon nitride product with surface area as high as 267.80 m²/g. Removal of water from the composite via solvent exchange with *t*-butanol was also found to be an effective way to prevent the collapse of porous structure.

REFERENCE

- [1] Lin, C. and Ritter, J. A. (1997). *Effect of synthesis pH on the structure of carbon xerogels*. Carbon. **35** (9), 1271-1278.
- [2] Choi, J.Y., Kim, C.H., et al. (1999). *Carbothermic Synthesis of Monodispersed Spherical Si₃N₄/SiC Nanocomposite Powder*. J. Am. Ceram. Soc. **82** (10), 2665-2671.

VITA

Mr. Kanoksak Luyjew was born on 10th October, 1982, in Nakhonsithammarat, Thailand. He received his Bachelor degree of Engineering with a major in Chemical Engineering from Prince of Songkla University, Songkhla, Thailand in March 2005. He continued his Master study in the major in Chemical Engineering at Chulalongkorn University, Bangkok, Thailand in June 2005.



สถาบันวิทยบริการ
จุฬาลงกรณ์มหาวิทยาลัย